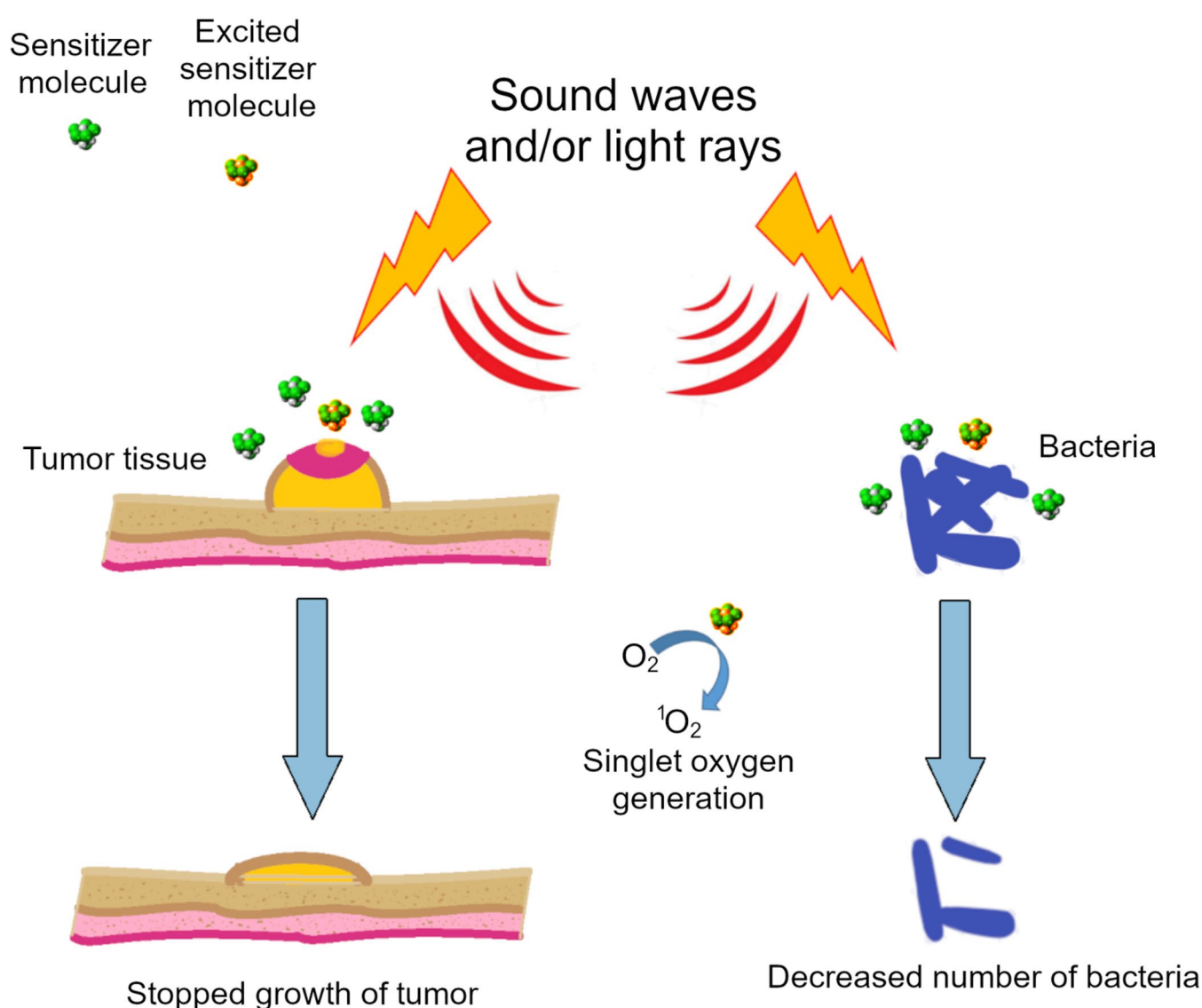


Special  
Collection

# Excited State and Reactive Oxygen Species against Cancer and Pathogens: A Review on Sonodynamic and Sono-Photodynamic Therapy

Marcin Wysocki,<sup>[a, b]</sup> Beata Czarczynska-Goslinska,<sup>[c]</sup> Daniel Ziental,<sup>[a]</sup> Maciej Michalak,<sup>[a]</sup> Emre Güzel,<sup>[d, e]</sup> and Lukasz Sobotta\*<sup>[a]</sup>

## Effect of photodynamic and sonodynamic therapy



Photodynamic and sonodynamic therapy are therapies having great potential in the treatment of bacterial infections and cancer. Their background is associated with photo- and sonosensitizers - substances that can be excited when exposed to light or ultrasound. These sensitizers belong to a various groups of compound, including porphyrins, porphyrazines, and phthalocyanines. Releasing the energy when returning to the ground state can occur in the manner of transferring it to oxygen molecules, leading to reactive oxygen species able to

disrupt membranes of bacterial and cancer cells, leaving the organism's cells unaffected. In recent years, the number of reports on numerous sensitizers being effective has been constantly growing. Therefore, the development of this field may prove beneficial for dealing with cancer and microbes. This review describes the development of photodynamic and sonodynamic therapy, as well as their combination, with emphasis on sonodynamic therapy and its potential in the treatment of cancer and bacterial infections.

## 1. Introduction

Cell proliferation is a life-crucial process, but due to its complexity, some abnormalities can occur. Although organisms tend to deal with them naturally, there is a chance that some cells get out of control and start to divide uncontrollably. This can lead to cancer, which is one of the most mortal diseases.<sup>[1]</sup> Treatment of cancer is always a difficult task because many types have different structures, properties, nature, and the ability to form metastasis, in most cases remaining untreatable, finally leading to death.<sup>[2]</sup> On the other hand, microbial infections remain a serious threat for many patients, thus combating bacteria becomes more than a current problem, due to the resistance phenomenon.<sup>[3-6]</sup> Drug resistance can be acquired by bacteria in many ways, mainly by increasing the production of enzymes or expressing efflux pumps, often associated with mutations and gene exchange performed among bacteria.<sup>[4-6]</sup> Popular examples of bacterial strains that became resistant to antibiotics dedicated for them are methicillin-resistant *Staphylococcus aureus* (MRSA) and *Escherichia coli* ESBL+ (extended-spectrum beta-lactamases), due to increased production of enzymes called "beta-lactamases".<sup>[4,6]</sup> These enzymes are able to decompose beta-lactam moiety present in the structure of methicillin and/or other antibiotics belonging to the beta-lactam group, such as penicillins, cephalosporins, or monobactams (Figure 1).<sup>[6]</sup>

After years of antibiotic abuse, this problem advanced and finally results in bacteria being invulnerable to conventional methods of treatment. These organisms are abbreviated as MDR (multi-drug resistant) and are extremely difficult to treat.<sup>[6]</sup> For this reason, it is now said about a "post-antibiotic era".<sup>[7]</sup> This is why there is an urge for discovering, designing, and developing new methods of treatment, either for bacterial infections or cancer. Good examples of the newest approach to this topic are therapies utilizing light or sound, called 'photodynamic therapy' (PDT) and 'sonodynamic therapy' (SDT) respectively. Both methods are often associated with compounds that are of natural origin, thus potentially decreasing the risk of such treatment.<sup>[4,8]</sup> Classic methods are more invasive and often involve the introduction of toxic and dangerous substances to cure. On the other hand, PDT and SDT rely on interactions of light or ultrasound (US) with sensitizers - compounds able to accumulate energy in a way of excitation.<sup>[9]</sup> Well-known examples of such substances are porphyrinoids (Figure 2), as well as dyes, i.e., Rose bengal, methylene blue, or popular food additives, such as curcumin.<sup>[4,10,11]</sup>

Molecules in an excited state can radiate this stored energy as light or transfer it to the oxygen molecule, leading to the generation of Reactive Oxygen Species (ROS). ROS includes different types of radicals such as hydroxyl radicals (HO<sup>•</sup>), superoxide anions (O<sub>2</sub><sup>•-</sup>), both types produced in a reaction called Type I and singlet oxygen (<sup>1</sup>O<sub>2</sub>), produced in Type II reaction. Both types involve the irradiation-induced transfer of the sensitizer's electron from the ground state into the excited state. The ground state for most compounds, including sensitizers is a singlet state when all electrons are paired, thus this state when excited, is not energetically favorable. The excited sensitizer becomes unstable and emits the energy as radiation (fluorescence or heat) or turns into an excited triplet state, more stable due to lower energy.<sup>[12-16]</sup> Type I process involves then the reaction between the triplet-state sensitizer


[a] M. Wysocki, D. Ziental, M. Michalak, Prof. L. Sobotta  
Chair and Department of Inorganic and Analytical Chemistry  
Poznan University of Medical Sciences  
Rokietnicka 3, 60-806 Poznan (Poland)  
E-mail: lsobotta@ump.edu.pl

[b] M. Wysocki  
Doctoral School  
Poznan University of Medical Sciences  
Bukowska 70, 60-812 Poznan (Poland)

[c] Dr. B. Czarzynska-Goslinska  
Chair and Department of Pharmaceutical Technology  
Poznan University of Medical Sciences  
Grunwaldzka 6, 60-780 Poznan (Poland)

[d] Prof. E. Güzel  
Department of Engineering Fundamental Sciences  
Sakarya University of Applied Sciences  
54050 Sakarya (Turkey)

[e] Prof. E. Güzel  
Biomedical Technologies Application and Research Center (BIYOTAM)  
Sakarya University of Applied Sciences  
54050, Sakarya (Turkey)

 This article belongs to the Early-Career Special Collection, "EuroMedChem Talents".

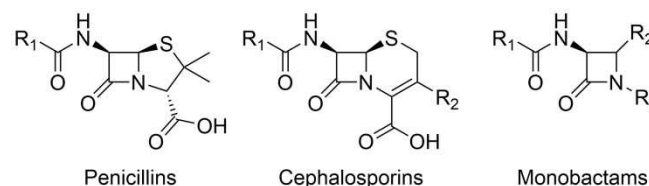


**Figure 1.** Structures of beta-lactam antibiotics; R<sub>1</sub> - mainly benzyl or aryl; R<sub>2</sub> - methyl or hydrogen; R<sub>3</sub> - sulfonic or carboxylic acid.

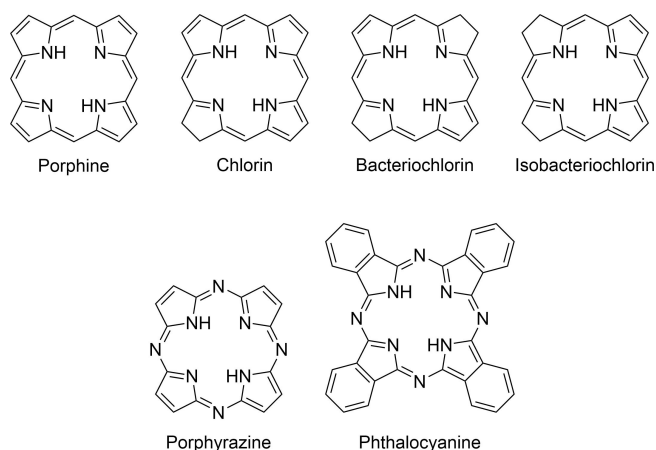
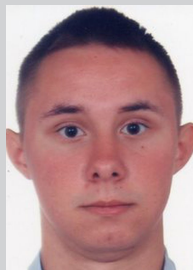


**Figure 2.** Structures of exemplary unsubstituted porphyrinoids.

and surrounding organic molecules, for example, cell components, turning both sensitizer and those molecules into radicals or radical ions. Both species can then react with molecular oxygen to generate oxygen-based radicals and anion radicals, although this is not necessary, thus Type I can be considered an oxygen-independent process. On the other hand, Type II involves the direct reaction between triplet-state sensitizer with oxygen, naturally having a triplet state as its ground state. This type of reaction tends to inverse the spin of electrons, therefore turning both sensitizer and oxygen into a singlet state. In this case, reactions with oxygen are necessary, and thus Type II is considered an oxygen-dependent process.<sup>[12–16]</sup> In both PDT and SDT Type II is considered the main type of ROS-generating reactions, although it can depend on the type of the sensitizers: organic ones tend to follow rather Type II, while inorganic ones can proceed Type I process.<sup>[15]</sup> Formed ROS are highly reactive and able to interact with groups present on membranes and cell walls, causing their disruption (Figure 3). ROS can also



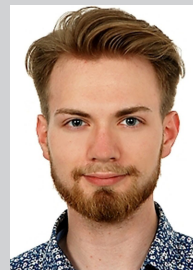
Marcin Wysocki is currently a PhD student in pharmaceutical sciences at Poznan University of Medical Sciences, under the supervision of Assoc. Prof. Lukasz Sobotta and Assoc. Prof. Emre Güzel. He received his MSc Eng. degree in chemical technology at Poznan University of Technology in 2021. His current research is based on porphyrinoids and their applications in antibacterial and anticancer photodynamic and sonodynamic therapy.



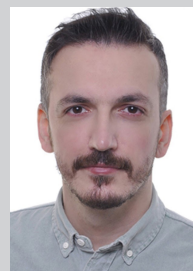
Beata Czarzynska-Goslinska PhD has been working at the Department of Pharmaceutical Technology at Poznan University of Medical Sciences. The scope of her research is mainly focused on the technology of solid and semi-solid drug forms, with the assessment of interactions between excipients or nanoparticles with selected pharmaceutically active substances. She has long-term experience in the pharmaceutical industry, where she was working as a formulator at the Research and Development Department of GlaxoSmithKline Pharmaceuticals in Poznan.



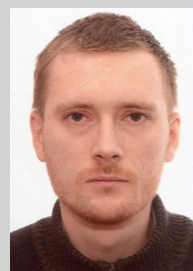
Daniel Ziental is a graduate and teacher of the Poznan University of Medical Sciences. His main research interests are focused on the development of alternative antimicrobial therapies, in particular PACT. In 2019, he completed an internship at the Autonomous University of Madrid in the group of Professor Tomas Torres, where he learned about the chemistry of porphyrinoids and macrocyclic compounds.



Maciej Michalak is currently a second-year student in the MPharm program at Poznan University of Medical Sciences. As an active member of the “Photochemistry of the Macrocyclic Molecules student’s research group” at the Chair and Department of Inorganic and Analytical Chemistry, he participates in research under the supervision of Assoc. Prof. Lukasz Sobotta, MPharm Daniel Ziental and MSc Eng. Marcin Wysocki.



Emre Güzel is currently Assoc. Prof. at Sakarya University of Applied Sciences. He received his MSc from İstanbul Technical University in 2011 and PhD from Sakarya University in 2016 in the area of amphiphilic and phthalocyanine/porphyrazine hybrid photosensitizers. During this period, he was a visiting researcher at Prof. Tomas Torres’s laboratory at the Autonomous University of Madrid in 2015. His research interests include the preparation and study of various photosensitizers based on phthalocyanines and their fundamental and applied investigations in molecular photovoltaics and photodynamic therapy.



Lukasz Sobotta is currently Assoc. Prof. at Poznan University of Medical Sciences (PUMS). He received his MSc in pharmacy from PUMS in 2008 and in 2009 engineer degree from Poznan University of Life Science in dietetics. In 2015 he received his PhD from PUMS in the area of phthalocyanine/porphyrazine photosensitizers, their physicochemical properties and biological activity (against viruses and cancer). During this period, in 2013 he was a visiting researcher at Prof. Jan Balzarini’s laboratory. In 2015 as a postdoc he joined Prof. Tomas Torres’s team at the Autonomous University of Madrid. Currently, he is involved in research on photochemical properties of various organic and inorganic photosensitizers for photodynamic and sonodynamic bacteria inactivation.

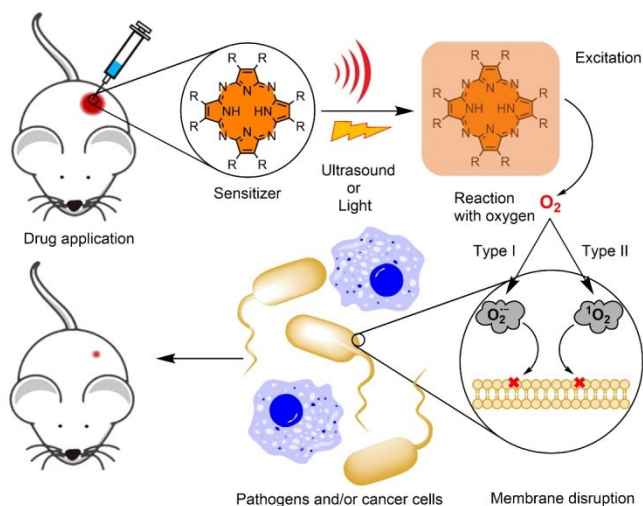


**Figure 3.** Simplified mechanism of PDT and SDT.

diffuse for a certain distance inside the cell and react with lipid membranes of their organelles or with components of cytosol, although for singlet oxygen the distance is several nanometers from sensitizer molecules, due to its short lifetime (10–320 nanoseconds).<sup>[12,14–17]</sup> Although ROS occur naturally in living organisms as by-products of the metabolism (except for singlet oxygen, formed only in plants due to photochemical activity of chlorophyll), as well as protective and signaling agents, their concentration within the organism is controlled by various antioxidants, including ROS scavengers to prevent cell damage. Typically, ROS scavengers include carotenes and tocopherols (mainly to quench singlet oxygen formed in plants), histidine, glutathione, and enzymes like superoxide dismutase. Thus it is important to consider sensitizers able to elevate ROS concentration high enough to overcome the capability of cells to degrade them and cause their death due to oxidative stress.<sup>[12,14,15]</sup> Unfortunately, there are some disadvantages of such an approach. PDT and SDT, as associated mainly with the generation of singlet oxygen, are dependent on oxygen availability in the environment, causing the efficiency of both methods to decrease in hypoxic conditions, typical for solid tumors, therefore providing useful methods of oxygen delivery may be crucial for elevating the efficiency of both methods.<sup>[18,19]</sup>

## 2. Photosensitizers Adapted for Sonodynamic Therapy

### 2.1. The basis of photodynamic therapy

Photodynamic therapy (PDT) has been known for over a century as an interdisciplinary therapeutic approach, which combines knowledge of chemistry, pharmacology, and physics, offering a valid alternative to fight tumors and antibiotic-resistant microbial infections.<sup>[3,11,20]</sup>

The general mechanism of PDT relies on the prior application of photosensitizer (PS) at the treated spot and its activation by light with appropriate intensity and wavelength. The activation of PS molecules results in the generation of singlet oxygen (or other ROS) which cause oxidative stress and ultimately cell death (necrosis) or programmed cell death (apoptosis).<sup>[11,20]</sup>

The long history of experiments and clinical trials allowed PDT to be developed over time, either by improving PS molecules or by upgrading and optimizing the delivery of light to targeted areas. Currently, there are three generations of PSs: the first being represented by Photofrin, the second containing chlorin or bacteriochlorin derivatives, and the third generation such as polyacrylamide or phthalocyanines.<sup>[9,21,22]</sup> The first and second generations of PSs are clinically tested and admitted to commercial use, while the third generation is still undergoing wide research.<sup>[23]</sup>

As mentioned before, to induce the therapeutic activity of PS molecules, a light at specific wavelengths needs to be applied to the targeted area. This process almost always takes place with the help of the lasers which are the most suitable light sources.<sup>[9]</sup> All strategies have their weak spot, in the case of PDT it's called "phototherapeutic window" and it refers to poor penetration of tissues by shorter wavelengths (< 650 nm) and the endogenous absorption of longer waves (> 850 nm), which results in the insufficient generation of singlet oxygen molecules. Thus the light used in PDT is generally within wavelengths ranging from 650 nm to 850 nm.<sup>[9]</sup> The most commonly used light sources are Argon/dye lasers, in the therapeutic range of 630 nm.<sup>[9]</sup>

### 2.2. Improving the therapeutic effect of sensitizers

PDT is an effective alternative for dealing with a wide range of microbes, especially antibiotic-resistant ones. SDT uses similar principles, and thus it is possible to share sensitizers between the two methods. These therapies can be used against both, Gram-positive and Gram-negative bacteria.<sup>[3,7,24]</sup> It is very promising in the "post-antibiotic era" as it brings an opportunity to efficiently deal with nosocomial infections related to surgical wounds etc.<sup>[25]</sup> The main bactericidal factor of PDT and SDT is the ability of the sensitizers to generate ROS that disrupt functions of organelles such as cell membrane, ribosomes, etc., and generally put bacteria into a state of oxidative stress.<sup>[14]</sup>

When considering PDT and SDT against microbes, there are two main concerns about sensitizers: their ability to generate singlet oxygen efficiently and the ability to get in the close neighborhood of the treated pathogen's structures e.g. cell membrane. Thus, sensitizers that are bonded with targeted bacteria, for example, sensitizers bearing several positive charges, such as tetrakis(1-methylpyridinium-4-yl)porphyrin tetraiodide **1** (Figure 4) together with high lipophilicity at their peripheries indicate better results despite being less efficient at generating singlet oxygen.<sup>[3,26–29]</sup> The inactivation of bacteria may be very effective, for instance, 2,3-bis((4-(3,5-bis(hydroxymethyl)butyl)tio)tribenzoporphyrine **2** (Figure 4)



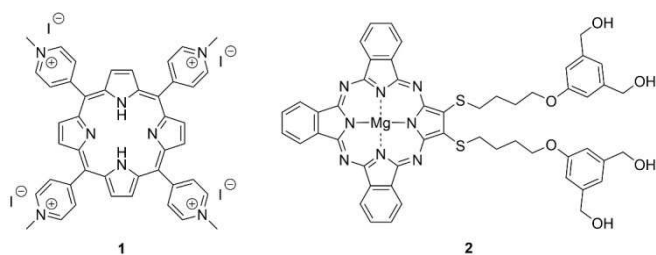


**Figure 4.** Structures of cationic porphyrin 1 and tribenzoporphyrazine derivative 2.

used against *S. aureus* represents the killing rate of over 5.9 log at a concentration of 10  $\mu\text{M}$  and under low light doses.<sup>[25]</sup> The PDT and SDT might be combined with antibiotic therapy resulting in increased disinfection efficacy on bacterial pathogens compared to monotherapies alone.<sup>[5,30–32]</sup> This multi-directional strategy may take advantage of a wide range of combinations of therapeutic compounds, such as bacterial cell membrane-targeting antibiotics, bacterial cell wall-targeting antibiotics, and bacterial protein synthesis-inhibiting antibiotics, bacterial nucleic acid synthesis-inhibiting antibiotics, multi-antibiotic combinations, and various sensitizer molecules.<sup>[5]</sup> Although the results vary depending on pathogens and applied combinations, in almost all cases there is a visible synergistic effect that favors the strategy.<sup>[5,7,10,33–35]</sup>

Anticancer PDT and SDT similarly take advantage of sensitizers' ability to generate singlet oxygen that causes damage and oxidative stress to tumor cells. As the tumor integrates with the organism by inducing angiogenesis to provide itself oxygen and nutrients, therefore the mechanisms involved in achieving therapeutic effect are somehow different from the inactivation of microbes.

The reactive oxygen damages cell structures by oxidizing biomolecules (mainly proteins). The result of all these events is the activation of numerous mediators inducing programmed cell death pathways (apoptosis) or rapid cell death (necrosis).<sup>[11]</sup> Usually, three main parameters are described concerning the anticancer activity of sensitizers: (a) accumulation of the molecules in tumors; (b) local illumination; (c) the presence of molecular oxygen in the tissue.<sup>[36]</sup> The main focus of the investigation of synthetic sensitizers is put on porphyrins, chlorins, bacteriochlorins, isobacteriochlorins, and phthalocyanines (Figure 2).<sup>[11]</sup>

Selective accumulation of sensitizer is a very complex process and varies depending on the used therapeutic agent and the type of targeted tumor, and still is not completely understood.<sup>[9]</sup> However, it can be improved by altering the sensitizers by introducing signaling molecules e.g. cancer cells consume much more glucose than the normal cells (the Warburg effect), thus selectivity is increased by synthesizing sugar-conjugated sensitizers.<sup>[23]</sup>

Another factor that contributes to the accumulation of sensitizer molecules in tumor regions and ultimately to its ablation is its neovasculature.<sup>[20]</sup> Additionally, the photodynamic or sonodynamic reaction affects blood vessels in the tumor

region, which as neovasculature are less durable. By disruption of their continuity, blood will not flow thus not providing nutrients and oxygen to the tumor, which will result in its further death.<sup>[20]</sup> The reaction may also enhance the immune response against malignancy, the direct effects on the tumor and its vasculature initiate an immune cascade of releasing inflammatory mediators.<sup>[12,15,39,42–45]</sup> This release stimulates and activates various white blood cells which converge in the treated area and significantly contribute to killing tumor cells.<sup>[20,42,43]</sup> Considering these three paths, PDT and SDT have a multifactorial impact on treating tumors. One of their effects is associated with the direct killing of tumor cells. The other one is causing their death due to damaging tumor vasculature. The last major one is rapid recruitment and activation of immune cells, favoring the development of anticancer adaptive immunity.<sup>[23]</sup> On the other hand, neovascular damage and hypoxia caused by PDT and SDT can result in increased expression of hypoxia-inducible factor HIF-1 $\alpha$ , which induces the transcription of genes and for example angiogenic growth factors, such as vascular endothelial growth factor (VEGF). The expression of angiogenic growth factors can result in recurrence of the tumor vasculature and the tumor itself.<sup>[46,47]</sup> Due to those facts, merging PDT and SDT with growth-factor targeting therapies can potentially increase the long-term therapeutic effects.<sup>[46,47]</sup> However, those effects are not related only to cancer.<sup>[48–50]</sup>

### 2.3. Strategies to achieve better targeting and delivery

There are other strategies such as introducing to the sensitizer structures charged or uncharged groups, increasing their solubility (hydrophilic, hydrophobic or amphiphilic), and linking them with nanostructures (liposomes, nanomicelles, nanoplasts, nanogels, or nanoparticles), to improve their targeting performance.<sup>[12,21,22,37,38]</sup> Due to the amphiphilic nature and the ability to enclose other molecules inside liposomal and micellar formulations, liposomes and micelles are commonly used to carry water-insoluble sensitizers into an aqueous environment and enhance their delivery. Liposomes consist of two opposite-oriented amphiphilic layers, while micelles consist of one layer only. The layers in both cases can be monomeric (phospholipids or classic surfactants, e.g. long-chain salts or quaternary ammonium compounds) and polymeric (having hydrophobic polymer block-like polycaprolactone or polylactic acid together with hydrophilic one like polyethylene glycol).<sup>[12,21,38]</sup> On the other hand, nanoparticles do not need to have distinguished hydrophobic and hydrophilic parts in their shells, therefore remaining undefined as liposomes or micelles. They consist mainly of hydrophilic polymers, forming stable colloidal dispersions with water and being often biocompatible (polyacrylamide, polyvinyl alcohol) and easily biodegradable. The other important property is the ability to release drugs in a controlled way.<sup>[22,37]</sup> The most common examples are silica nanoparticles, quantum dots, fullerenes, metal oxides, and metals themselves. Silica nanoparticles are often used as mesoporous carriers, having a great encapsulation capacity, due to high both surface

area and porous volume. Although quantum dots are often conjugated with various sensitizers, they can be used directly in PDT and SDT. Fullerenes can take part in both Type I and Type II reactions, depending on the environment – in aqueous conditions hydroxyl radicals-generating Type I predominates, while under hydrophobic conditions Type II becomes the main one. Zinc and titanium oxides are widely used as photocatalysts, thanks to their ability to become excited by UV radiation and generate radicals in reaction with water or oxygen. Despite the great potential of titanium dioxide in PDT, it has some important drawbacks, such as excitation only under harmful UV radiation (avoidable by using SDT), having also poor tissue penetration, and overheating under irradiation. Therefore, it must be accompanied by other molecules in order to enhance its safety. Metal nanoparticles are most often associated with gold nanoparticles, possessing several useful properties, such as easy surface modification and the preference to accumulate in tumor sites.<sup>[9,12,17,39–41]</sup>

#### 2.4. There's more

The perspectives for the development of PDT and SDT are ranging from designing new generations of sensitizers, improvement of administration methods, innovating better ways of light delivery, and searching for novel applications of therapies themselves. To meet these demands, researchers come up with different strategies concerning the delivery of the drug e.g. poly(acrylamide) nanoparticles, micelles or liposomes, monoclonal antibodies, increasing hydrophilic character, and altering molecules with additional structures such as sugars.<sup>[3,21–23]</sup>

As the PDT and SDT are very versatile strategies, their new applications mainly focus on combining them with other therapies such as chemotherapy or changing a perspective for one of the concepts mentioned above like the delivery of sensitizers. The combination of PDT and SDT with antibiotics or with anticancer drugs achieves significantly better results in comparison to these methods used separately.<sup>[5,9]</sup> For increased selectivity, combinations with immunotherapy were developed. It relies on the specificity of the antibody chemicals which are joined to a photo absorbing molecule that absorbs light in near-infrared lengths of the spectrum.<sup>[23]</sup>

### 3. Sonodynamic Method

#### 3.1. Treatment-helping ultrasounds

Ultrasounds (US) have been widely used for years and became a real friend of modern medicine. Due to the ability of deep penetration of tissues and the possibility of focusing the irradiation onto a small region, US can be used not only for ultrasonography imaging but also for treatment.<sup>[7,8,24,31,32,51]</sup> The US can increase the permeability of cell membranes, thanks to the sonoporation, allowing the exchange of substances through the cell membranes for a short period, making a possibility

either to activate drugs or enhance their uptake.<sup>[8,32]</sup> Similar phenomenon can be used in drug delivery through the skin on the way of sonophoresis. Other applications of US can be associated with surgery and dentistry (ultrasound scalpel, bone cutting, and endodontic irrigation), as well as disruption of blood clots.<sup>[8]</sup> What is more, the US can be helpful in physiotherapy and have also the ability to induce apoptosis and the treatment is often characterized by low cost and safety.<sup>[7,8,52]</sup>

#### 3.2. Mechanism of sonodynamic therapy

Sonodynamic therapy (SDT) is a non-invasive therapeutic modality that provides high tissue penetration by triggered ultrasound (up to 10 cm).<sup>[53,54]</sup> Similar to PDT, sonosensitizer (SS) molecules are activated to generate cytotoxic ROS such as HO<sup>•</sup> and <sup>1</sup>O<sub>2</sub>.<sup>[55]</sup> A particularly effective SS is a prerequisite for SDT. Compared to PDT, SDT can overcome the problems of tissue penetration and phototoxicity.

The biological effects of SDT are mainly associated with mechanical, thermal, and cavitation influence.<sup>[15,24,32,56]</sup> Thermal effects include absorption of US energy and further its dissipation, leading to elevation of temperature and thus possible deactivation of enzymes.<sup>[56–58]</sup> Mechanical effects include changes in cell membrane permeability, as well as mechanical rupture of membranes and cell agglomerates.<sup>[56,59]</sup> The increased permeability can enhance the uptake of sonosensitizer (SS), resulting in its higher activity.<sup>[32,60]</sup> Cavitation effects rely on creating microbubbles, which naturally oscillate in response to the present US. While the intensity of the US is relatively low, the bubbles remain stable and do not tend to collapse. This phenomenon is known as stable (non-inertial) cavitation. On the other hand, higher intensities tend to provide unequal oscillations of bubbles, thus making them collapse (inertial cavitation), elevating the temperature and pressure up to few thousand K and hundreds of MPa respectively.<sup>[8,57,58,61,62]</sup> Additionally, mechanical stress generated by cavitation can result in leakage of intercellular components, due to shock and damage to cell membranes.<sup>[63]</sup> Another important factor is the production of ROS, due to various phenomena accompanying the occurrence of US, such as excitation of SSs, followed by the respective release of energy when returning to the ground state. There are several mechanisms proposed and most of them are associated with acoustic cavitation.<sup>[8,24,57]</sup> One of the proposed mechanisms follows the pathway that the SS, water, and other moieties inside the cavitation bubble undergo pyrolysis or thermal decomposition. This leads to the formation of free radicals, which are then able to react with dissolved oxygen and form ROS.<sup>[8,15,24,56,57,61]</sup> The second one is explained by excitation of SS performed by sonoluminescence, being flashes of light occurring as a side effect of inertial cavitation.<sup>[8,24,61,64]</sup> The excited SS is then able to transfer its stored energy to an oxygen molecule, resulting in ROS formation, either in a Type I process (forming radicals) or in a Type II process (leading to singlet oxygen).<sup>[8,15,24,57,60,61,64–66]</sup> It should be remembered that for inorganic species such as metal oxides, the mechanism is

associated mainly with the occurrence of electron-hole pairs.<sup>[65]</sup> Mechanical waves of the US can induce the transition of an electron. The electrons and holes are then separated and can recombine, therefore migrating to the surface of SS.<sup>[65,67]</sup> Depending on the type of SS, different mechanisms or combinations of them can occur. There is a possibility that one universal mechanism exists and we are simply unable to determine it at the moment, nevertheless, the chances of such occurrence are relatively low. For this reason, all of the mentioned mechanisms of sonodynamic action are possible to indicate, thus they are generally accepted.<sup>[8]</sup>

### 3.3. Against bacterial infections

Although the first hypothesis indicating the possibility of sonodynamic approach in treating bacterial infections has been reported in 2009,<sup>[51]</sup> this method has not been widely examined

yet. It seems that Gram-negative bacteria are less susceptible to these kinds of therapy, but some exceptions do not follow the general rule (Table 1).<sup>[7]</sup> Another aspect of treating bacterial infections is the ability of bacterial strains to form a biofilm, being a difficult, because of increased resistance to many agents, acting as a physical barrier.<sup>[68,69]</sup> Bacteria forming biofilm can produce increased amounts of polysaccharides, leading often to the appearance of plaques, as well as contamination of surfaces such as medical devices or teeth, which are often difficult to remove completely, even with mechanical methods.<sup>[69,70]</sup> Due to this phenomenon, the evaluation of sonodynamic methods should be also investigated towards the eradication of bacterial biofilm, for avoiding potential difficult-to-treat infections caught during regular treatment of patients.<sup>[69]</sup>

Firstly, the US was used to enhance the activity of antimicrobial drugs (Figure 5). Liu *et al.* in 2011 investigated whether there is a synergy between the US and the use of

**Table 1.** The efficiency of different sonodynamic approaches in treating bacteria.

Strain	SS and concentrations (calculated for drug)	US parameters	Duty cycle	Irradiation time	Power density [J/cm <sup>2</sup> ]	Reduction	Ref.
<i>E. coli</i>	Ciprofloxacin 3 (30 μM)	40 kHz, 1 W/cm <sup>2</sup>	100 %	30 min	1800	0.78 log (83 %)	[31]
	Levofloxacin 4 (28 μM)			30 min	1800	1.7 log (98 %)	
<i>M. smegmatis</i>	Levofloxacin 3 (0.7 μM)	42 kHz, 0.329 W/cm <sup>2</sup>	100 %	20 min	394.8	0.92 log (88 %) <sup>[a]</sup>	[32]
<i>E. coli</i>	Rose Bengal 5 (15 μM, <i>E. coli</i> )	28 kHz, 0.84 W/cm <sup>2</sup>	100 %	60 min	3024	4.7 log	[24]
<i>S. aureus</i>	(5 μM, <i>S. aureus</i> )				3024	5.99 log	
<i>P. aeruginosa</i>	Rose Bengal 5- C(KLAKLAK)2 (10 μM)	1 MHz, 3 W/cm <sup>2</sup>	50 %	6 min	1080	7 log	[7]
<i>S. aureus</i>	Curcumin 7 (40 μM)	1 MHz, 1.56 W/cm <sup>2</sup>	100 %	10 min	1800	5 log	
<i>S. aureus</i>				5 min	468	5 log	[52]
<i>B. cereus</i>	Curcumin 7 (2 μM)	1 MHz, 1.56 W/cm <sup>2</sup>	100 %	3 min	280.8	5.6 log	[71]
<i>E. coli</i>	Curcumin 7 (50 mM)	1 MHz, 1.56 W/cm <sup>2</sup>	[a]	5 min	468	2 log	
<i>S. mutans</i>				1 min	93.6	3 log (99.9 %)	[62]
<i>E. coli</i>	Propyl gallate 8 (10 mM)	40 kHz, 0.092 W/mL	100 %	30 min	165.6 [J/mL]	6 log	[63]
<i>L. innocua</i>	Hypocrellin B 9 (40 μM)	1 MHz, 1.56 W/cm <sup>2</sup>	100 %	45 min	248.4 [J/mL]	6 log	
<i>S. epidermidis</i>				5 min	468	4 log	[70]
<i>S. aureus</i>	Hypocrellin B 9 (40 μM)	1 MHz, 1.56 W/cm <sup>2</sup>	100 %	5 min	468	5 log	[72]
<i>L. innocua</i>						5 log	[73]
<i>S. mutans</i>	ZnO, TiO <sub>2</sub> (31 μM)	1 MHz, 2 W/cm <sup>2</sup>	[a]	1 min	120	7.9 log	[69]
<i>S. aureus</i>	HMME 10 (82 μM)	1 MHz, 6 W/cm <sup>2</sup>	30 %	30 min	10800	1.3 log (95 %)	[74]
<i>P. gingivalis</i>	HMME 10 (65 μM)	1 MHz, 3 W/cm <sup>2</sup>	30 %	10 min	1080	4.7 log	[64]
<i>E. coli</i>	Chlorin e6 11 (20 μM)	1 MHz, 1.56 W/cm <sup>2</sup>	100 %	4 min	374.4	2 log	[60]
<i>S. aureus</i>						7 log	
<i>E. coli</i>	Purpurin-18 12 (20 μM)	1 MHz, 0.97 W/cm <sup>2</sup>	100 %	5 min	291	0.5 log (70 %) <sup>[a]</sup>	[35]
<i>S. aureus</i>						1.3 log (95 %) <sup>[a]</sup>	
<i>S. aureus</i>	TCPP 13 (63 μM)	1 MHz, 0.97 W/cm <sup>2</sup>	50 %	8 min	465.6	~ 100 % <sup>[a]</sup>	[75]
<i>S. aureus</i>						3.15 log (99.93 %)	[67]
<i>S. aureus</i>	DVDMS 14-TiO <sub>2</sub> (0.83 μM)	1 MHz, 3 W/cm <sup>2</sup>	100 %	1 min	180	1.12 log (92.41 %)	[65]

[a] Exact data were not provided.

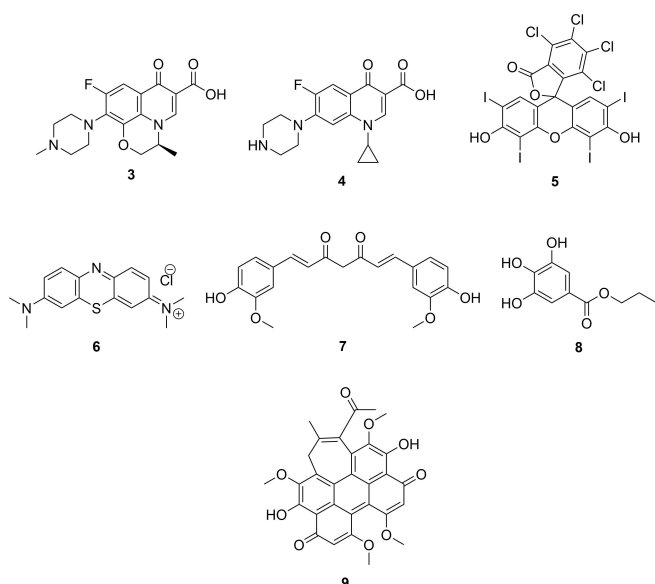


**Figure 5.** Structures of non-porphyrinoid SSs.

levofloxacin **3** or ciprofloxacin **4** (Figure 5) *in vitro* against the colonies of *E. coli* in presence of US at the frequency of 40 kHz and 1 W/cm<sup>2</sup> of power density.<sup>[31]</sup> The experiment has shown a significant enhancement in inhibitory ratios for both drugs during US irradiation. For this reason, Liu *et al.* have also performed further examination with different concentrations of both antibacterial agents, different times of US irradiation, and different temperatures. The best results were observed for the concentration of 10 µg/mL (compared with 6 µg/mL and 8 µg/mL) of **3** and **4** combined with US irradiation, showing the inhibitory ratios of 98% (1.7 log) and 83% (0.78 log) respectively. General observations have shown better activity of **3** in every case. Liu *et al.* also suggested that the best synergy between **3** or **4** and US comes with elongation of irradiation time from primary 15 min to half an hour. Further elongation (up to 45 min) of irradiation time did show enhanced activity only for **4**. Additionally, Liu *et al.* also investigated the influence of medium temperature *in vitro* and the results have shown that the temperature of 30 °C was much more beneficial than 20 °C. In opposition, a further increase of temperature to 40 °C did not show any significant changes in inhibitory ratios. Liu *et al.* also investigated the amount of ROS generated by **3** and **4** in the presence of US. The samples have contained the diphenylcarbazide as a chemical quencher of ROS. Concentrations of both drugs varied from 10 to 50 µM and as expected, higher concentrations of both drugs resulted in higher ROS generation after 1 h of sonication, although quantum yields were not given. Additionally, examination of various irradiation times (15, 30, 45, and 60 min respectively), shows that ROS generation increases significantly over time. In both cases, **4** was more effective SS than **3**. Liu *et al.* tried also to identify ROS generated by both drugs, using various quenchers: sodium azide (for identification of singlet oxygen), vitamin C, and butylhydroxytoluene (both for identification of superoxide and

hydroxyl radicals). After 1 h of irradiation, quenching rates in the presence of sodium azide were lower than for the other ones. These have indicated that under the US mentioned antibiotics follow mainly Type I mechanism of sonodynamic process (generation of radicals).<sup>[31]</sup> Another approach to **3** in the role of SS has been performed by Dong *et al.* in 2017.<sup>[32]</sup> The investigation was aimed to treat *Mycobacterium smegmatis*, the surrogate of *Mycobacterium tuberculosis*. At first, the activity of raw US was tested against bacteria. The frequency was established at 42 kHz, while the intensity of US and irradiation time was varied (0.138 W/cm<sup>2</sup> and 0.329 W/cm<sup>2</sup> with 5 or 20 min of irradiation). Both approaches using the lower intensity, as well as irradiation with higher intensity for 5 min, showed no significant activity, however, after 20 min of irradiation around 21.4% (0.1 log) reduction in cells occurred. Then, the effects of US combined with an antibacterial drug over time have been examined. The tests show that **3** both alone and with US treatment had an inhibiting effect on *M. smegmatis*. Additionally, a comparison of **3** activities in various concentrations (0.125 mg/L and 0.25 mg/L), shows that the reduction of bacterial viability increased with concentration, reaching approx. 80% (0.7 log) and 88% (0.92 log), with US and 70% (0.52 log) and 75% (0.6 log) without US, respectively.<sup>[32]</sup>

Another class of compounds gladly used to investigate their sonodynamic activity are dyes. Nakonechny *et al.* in 2013 investigated the influence of Rose bengal **5** (RB, Figure 5) with an US irradiation against *S. aureus* and *E. coli*, representing Gram-positive and Gram-negative bacteria respectively.<sup>[24]</sup> The US frequency was set at 28 kHz and the intensity of irradiation was 0.84 W/cm<sup>2</sup>. The whole experiment was performed for an hour at a temperature of 10 °C and in the dark, to avoid eventual photodynamic excitation. The concentrations of **5** were established at 5, 10, and 15 µM for combat of *E. coli* and 1.5, 3, and 5 µM for *S. aureus*. **5**-mediated SDT resulted in a significant reduction of *E. coli* (up to 4.7 log reduction for 15 µM) and *S. aureus* (up to 5.99 log reduction for 5 µM). In comparison to treatment without the US, **5** did not show any significant influence on the *E. coli*, while for *S. aureus* the activity of **5** was still significant, reaching up to 2.4 log for 5 µM. Additionally, Nakonechny *et al.* investigated the activity of methylene blue **6** (MB, Figure 5) against *S. aureus* only. The study shows that even the concentration of 30 mM was insufficient for **6**-mediated SDT, reaching at best only 1.7 log reduction.<sup>[24]</sup> Costley *et al.* in 2017 also investigated the influence of **5** modified with a peptide and activated with a US irradiation, on the viability of *S. aureus* and *P. aeruginosa*.<sup>[7]</sup> The modification of **5** was prepared by attaching an octanoic acid moiety through the esterification of **5** with 8-bromooctanoic acid. Then the product of this reaction was coupled with a synthesized peptide called C(KLAKLAK)<sub>2</sub>, forming an amide. C(KLAKLAK)<sub>2</sub> is an abbreviation for an antimicrobial and proapoptotic peptide, where C stands for Cysteine, K for Lysine, L for Leucine, and A for Alanine, therefore forming the following sequence: Cys-Lys-Leu-Ala-Lys-Leu-Ala-Lys-Lys-Leu-Ala-Lys-Leu-Ala-Lys. The obtained compound was further investigated as a bactericidal agent following excitation with 1 MHz US and 3 W/cm<sup>2</sup> of power density in 50% duty cycle. First part of the



experiment on the activity of the obtained compound concerned the measurement of generated ROS given as changes of 1,3-diphenylisobenzofuran (DPBF) absorbance. The study shows that the presence of a peptide moiety in the structure of the compound does not decrease an amount of ROS generated under US irradiation. Further studies were performed to evaluate the impact of modification of RB on its bactericidal activity. The irradiation times were: 10 min for *S. aureus* and 6 min for *P. aeruginosa*, designated as optimal values for US of mentioned parameters (frequency and power). It was indicated that US and peptide-modified **5** (10  $\mu\text{M}$ ) separately presented a minor reduction for *S. aureus* (0.5 log and 1 log respectively) and, interestingly, 0.5 log and 3.5 log respectively for *P. aeruginosa*. For combined peptide-**5** with US the reduction was significant: 5 log for *S. aureus* and 7 log for *P. aeruginosa*, denying the consideration that Gram-negative bacteria are less vulnerable to SDT. This phenomenon consisting of an interaction between the positive-charged peptide chain and negative-charged cell wall has been described by Costley *et al.* Additionally, Costley *et al.* have shown that 5 min of US irradiation before the treatment could be beneficial due to enhancing SS diffusion into *P. aeruginosa* biofilm. The increased biofilm uptake was improved near 2-fold during the first 5 min of treatment, reaching up to 2.6-fold increase after 30 min.<sup>[7]</sup>

Even the use of antioxidants, such as curcumin **7** (CUR, Figure 5), which is also a popular food additive, could be applicable in SDT, as shown by Wang *et al.* in 2014.<sup>[52]</sup> They investigated the activity of **7** under US irradiation against MRSA. First tests were performed in the dark to obtain results of toxicity of **7** itself. Bacteria were incubated for 0–24 hours with **7** at concentrations of 0.5–500  $\mu\text{M}$ , showing that there was no bacterial growth reduction by **7** alone. Investigation of MRSA antibacterial effect was performed with a frequency of 1 MHz and 1.56 W/cm<sup>2</sup> of power density. The concentration of **7** was in the range of 2.5–40.0  $\mu\text{M}$  and the time of irradiation was 5 min. The results show that the combination of **7** and ultrasound had a significant effect on colony counts only for concentrations higher than 10  $\mu\text{M}$ . According to this, the best result (5 log reduction) was obtained for 40  $\mu\text{M}$  of **7**. Additional analysis of bacterial uptake was performed, indicating that 50 min is an optimal time for efficient **7** uptakes into studied cells.<sup>[52]</sup> Wang *et al.* continued the research and investigated the effect of **7** combined with the US against *B. cereus* and *E. coli*.<sup>[71]</sup> The **7** uptake by *B. cereus* over time was steady, while for *E. coli* the uptake was changing over time. The optimal time for both bacterial uptakes was identified as 50 min. Interestingly, for *B. cereus* the uptake after 50 min remained steady, whereas in the case of *E. coli* after this time the uptake significantly decreased. In the assessment of SDT potential, the frequency was set at 1 MHz with 1.56 W/cm<sup>2</sup> of power density, and **7** concentrations varied from 0.125 to 2  $\mu\text{M}$  for *B. cereus* and from 2.5 to 40  $\mu\text{M}$  for *E. coli*. The study shows that in the case of *B. cereus* neither **7** nor the US alone affected the bacteria viability, while for *E. coli* US had an insignificant effect. For both strains combination of **7** with the US presented a significant reduction in viability. Reduction of the colony count of *B. cereus* by 5.6 log was achieved, while for *E. coli* the effect was significantly lower – 2

log.<sup>[71]</sup> Also, there were some approaches utilizing **7** loaded into nanomicelles against *Streptococcus mutans*, a Gram-positive bacteria.<sup>[62]</sup> The loading of **7** assumed encapsulation in phosphatidyletanolamine modified with poly(ethylene glycol) nanomicelles (NM). The investigation of **7** NM was performed under 1 MHz frequency and 1.56 W/cm<sup>2</sup> of power density. The concentration of **7** and **7** loaded in NM was 50 mM. The activity of NM-loaded **7** under US irradiation was significantly higher than unloaded CUR, reaching 99.9% (3 log) and 90.8% (1.03 log) reduction, respectively. Pourhajbagher *et al.* also investigated the uptake of NM-loaded and unloaded **7** over time after certain intervals (5, 10, 30 min, 1 h, and 6 h), showing that the uptake of NM-loaded and unloaded **7** was quite similar in tendencies, whilst the uptake of NM **7** was slightly higher. The optimal time designated for uptake was in both cases 1 hour, after which the concentration of **7** started to decrease.<sup>[62]</sup> The use of food-grade antioxidants is not restricted for CUR, as shown in the example of propyl gallate **8** (PG, Figure 5), utilized by Nguyen Huu *et al.* against Gram-positive *Listeria innocua* and Gram-negative *E. coli*.<sup>[63]</sup> The investigation was performed with US having frequency of 40 kHz and a power density of 0.092 W/mL. The times of irradiation were different for both strains and varied from 5 to 30 min for *E. coli* and from 10 to 45 min for *L. innocua*. Concentration of **8** was established at 10 mM, showing that US alone had no antibacterial effect. Although, the **8** itself presented slight reduction of *E. coli* viability, reaching approximately 1 log reduction after 30 min. On the contrary, for *L. innocua*, **8** had no visible effect. Although the combination of US and PG resulted in 6 log reduction of both strains, even before reaching the time of 30 min. Nguyen Huu *et al.* investigated also the damage caused by **8** to the cellular membrane, showing that for *E. coli* 5 and 30 min of US irradiation alone had no significant effect, but for *L. innocua* there was a nearly 2-fold increase in membrane disruption after 45 min, in comparison to 10 min of irradiation. In contrast, **8** in both cases showed significant activity in cell membrane disruption, which for *E. coli* was elevated slightly when irradiated for 5 min and more rapidly when the irradiation time was established at 30 min. On the other hand, for *L. innocua* US alone had in both cases higher activity than **8**, while combining them resulted in the dramatic increase of cell membrane permeability after 45 min, compared to slight increase after 10 min of irradiation.<sup>[63]</sup>

There are also reports utilizing the agents considered antifungals for eradicating bacteria. Wang *et al.* used US-enhanced hypocrellin B **9** (HYP, Figure 5) against *Staphylococcus epidermidis*.<sup>[70]</sup> The frequency of US irradiation used by Wang *et al.* was 1 MHz, with a power density of 1.56 W/cm<sup>2</sup>. The experiment was led for 5 min and the highest effect was observed at a concentration of 40  $\mu\text{M}$ , resulting in 4 log reduction of bacteria viability, which was similar to an effect of vancomycin. In addition, **9** alone had no antibacterial effect. Wang *et al.* also determined the generation of ROS inside bacterial cells under US irradiation and indicated that the effect of combined **9** and US was much greater (22%) in comparison to untouched cells (2.2%). **9** and US used separately inhibited bacterial growth, 4% and 5.9% respectively.<sup>[70]</sup> Wang *et al.* have

continued their studies on **9** and they have performed experiments with *MRSA*.<sup>[72]</sup> The first part of the investigation was to determine the toxicity of **9** itself on *MRSA*. The concentration of SS varied from 0.5  $\mu\text{M}$  to 500  $\mu\text{M}$ , showing no significant reduction in bacteria viability, even after 24 hours. Further, the uptake of **9** in *MRSA*, with the concentration of the compound established at 50  $\mu\text{M}$ , while the time varied from 10 to 70 min was investigated. The uptake reached a maximum after just 10 min, but then started to decrease, reaching a minimum after 40 min. Afterward, the uptake started to increase, reaching a plateau after 50–60 min, thus the optimal time was designated as 50 min. The viability of the cells under US (1 MHz and 1.56  $\text{W}/\text{cm}^2$ ) combined with **9** was measured with the concentration of the compound varying from 2.5 to 40  $\mu\text{M}$ . It turned out that **9**, as well as the US alone, did not affect the viability of the cells. However, the combination of them resulted in a significant reduction of bacterial growth, up to 3 log for 20  $\mu\text{M}$  and 5 log for 40  $\mu\text{M}$  of SS.<sup>[72]</sup>

Although the metals are often linked with organic compounds, there are also approaches utilizing pure metal oxides, such as zinc oxide (ZnO), shown by Dolan *et al.*, against *L. innocua*.<sup>[73]</sup> The US frequency was adjusted to 20 kHz and the power was 43–45 W (from probe having 1,27 cm diameter, which gives then approximately 34.7  $\text{W}/\text{cm}^2$ ), while the concentration of ZnO was established at 20 to 40 mM and the time of irradiation was up to 20 and 12 min respectively. The study showed that the reduction of bacterial growth was achieved up to 5 log for 40 mM (after 8 min) and approx. 4 log for 20 mM after 20 min. The ZnO alone required higher concentration, and even in 128.8 mM, its reduction of cell viability reached approx. 1 log, while the reduction for the US alone was up to 1.8 log after 20 min.<sup>[73]</sup> ZnO was also utilized in comparison and combination with titanium dioxide ( $\text{TiO}_2$ ) by Pourhajibagher *et al.* against *S. mutans*.<sup>[69]</sup> Firstly, they measured the uptake of nanoparticles by bacteria for time-varying from 1 to 15 min. This showed similar tendencies for all three types of nanoparticles, that for the first 3 min the nanoparticles were taken rapidly, then the uptake significantly decreased, finally reaching a plateau after 5 min. Pourhajibagher *et al.* also investigated an antibacterial effect of the nanoparticles with concentrations varying from 0.3 to 200  $\mu\text{g}/\text{mL}$ . The study showed that without US irradiation, the higher concentration of nanoparticles had better antibacterial activity, although the higher the concentration, the less significant differences were visible. In comparison,  $\text{TiO}_2$  nanoparticles had the lowest impact on cell viability. Further investigation was associated with measurements of the antibacterial effect of US alone under 1 min of 1 MHz irradiation and with power density varying from 0.25 to 2  $\text{W}/\text{cm}^2$ . The investigation shows that the US alone had negligible antibacterial effect, 49% (0.3 log) for the highest intensity, although the intensity of 0.75  $\text{W}/\text{cm}^2$  was chosen as optimal. Finally, the antibacterial effect of nanoparticles with and without the US was compared. The study showed that nanoparticles combined with the US presented much higher efficiency than nanoparticles alone, especially mixed  $\text{TiO}_2/\text{ZnO}$  nanoparticles, reaching at 25  $\mu\text{g}/\text{mL}$  a 7.9 log reduction (similar to 0.2% chlorhex-

idine), while  $\text{TiO}_2$  nanoparticles and ZnO nanoparticles reached 5.8 log at 1.5  $\mu\text{g}/\text{mL}$  and 6.3 log at  $\mu\text{g}/\text{mL}$  respectively.<sup>[69]</sup>

Great interest in treatment based on the excitation of the molecules arouses porphine derivatives, such as porphyrins. Zhuang *et al.* tested the activity of hematoporphyrin monomethyl ether **10** (HMME, Figure 6) with US treatment against *S. aureus*.<sup>[56]</sup> The research was led with US frequency of 1 MHz, a power density of 6  $\text{W}/\text{cm}^2$  and 30% duty cycle. The concentration of **10** was in the range of 10–50  $\mu\text{g}/\text{mL}$ . The study indicated that a higher concentration of **10** under US irradiation had better antimicrobial effect, reducing the bacteria viability within 30 min up to 95% (1.3 log) for 50  $\mu\text{g}/\text{mL}$ . This concentration was used for further studies, investigating the influence of US intensity (power density). The examination was performed using power density varying from 1 to 6  $\text{W}/\text{cm}^2$  and indicated that under 2  $\text{W}/\text{cm}^2$  neither US nor US with **10** exerted a significant effect. For higher intensities, the viability reduction rate started to increase. The effect for the US alone was rather slight, eradicating at the highest value of power density about 38% of bacteria. In the case of **10** excited with the US, there was an increase in the eradication of bacteria at 3 and 4  $\text{W}/\text{cm}^2$  of power density, which increased more while the power density was set at 5 and 6  $\text{W}/\text{cm}^2$ , eradicating at best 95% (1.3 log) of bacteria. In addition, Zhuang *et al.* investigated the impact of **10** alone, measuring its dark toxicity against *S. aureus*. They showed that even 50  $\mu\text{g}/\text{mL}$  of **10** alone had no significant impact on the bacteria viability.<sup>[74]</sup> The bactericidal potential of US excited **10** was tested also against *Porphyromonas gingivalis*.<sup>[64]</sup> The investigation was led with 1 MHz ultrasound at 3  $\text{W}/\text{cm}^2$  power density and 30% duty cycle and the concentration of **10** varied from 10 to 40  $\mu\text{g}/\text{mL}$ . The study showed that a higher concentration of **10** had a better antibacterial effect and after 10 min of irradiation the reduction of bacteria viability achieved 4.7 log. Simultaneously, **10** alone did not affect the bacteria viability. Moreover, Zhang *et al.* investigated the influence of irradiation time on the effects of US combined with **10**. The concentration of **10** was established at 40  $\mu\text{g}/\text{mL}$ , providing the best results, and the time varied from one to ten min. Longer irradiation time resulted in higher efficiency, but

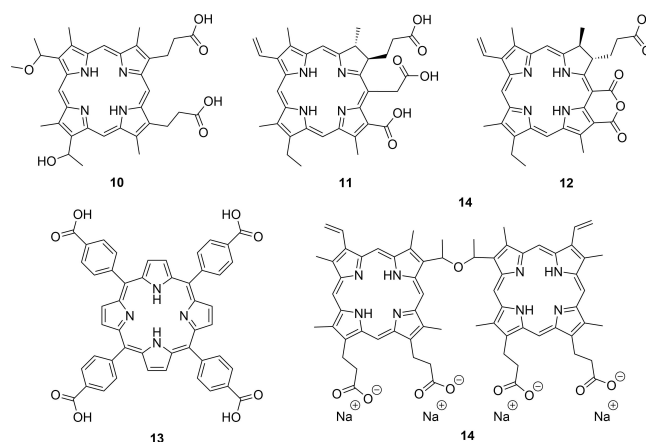


Figure 6. Structures of porphyrinoid SSs.

for the first 2 min, it was insignificant, then started to increase rapidly (up to 2.9 log reduction for 6 min and 4.7 log for 10 min), as compared with the US alone, which efficiency increased rather slightly over time.<sup>[64]</sup> Another example of porphyrinoids is chlorin e6 **11** (Ce6, Figure 6), investigated against *S. aureus* and *E. coli* by Xu *et al.*<sup>[60]</sup> US irradiation had a frequency of 1 MHz and 1.56 W/cm<sup>2</sup> of power density, while the concentration of **11** varied from 1.25 to 20 μM. The experiment indicated that the compound combined with the US after 15 min irradiation had no significant activity for SS concentrations lower than 2.5 μM. In contrast, higher concentrations resulted in a significant reduction in cell viability up to 7 log for *S. aureus* 11 2 log for *E. coli*. Additionally, without US irradiation even the highest concentration of **11** had no antibacterial effect, as well as the US alone had no impact on bacterial cells viability.<sup>[60]</sup> Another approach is associated with the enclosing of porphyrins in liposomes, which can be further modified to provide better targeting under systemic administration. Such an idea was investigated by Pang *et al.*, who used the modified liposome containing purpurin-18 **12** (PUR, Figure 6), against MRSA and *E. coli ESBL +*.<sup>[35]</sup> **12** was enclosed inside liposome vehicles consisting of cholesterol modified with maltohexaose, which delivered a specific targeting of bacteria. The targeting was achieved due to recognition by bacterial maltodextrin transporters. The studies were led under irradiation with the US at 1 MHz frequency and 0.97 W/cm<sup>2</sup> for 5 min. Firstly, the generation of singlet oxygen by **12** in liposomes was determined, as decay in dimethylanthracene fluorescence. The study shows also that **12** without US irradiation revealed no significant production of singlet oxygen. Further studies were associated with determination of **12** release, in comparison to enzyme-induced (Phospholipase A<sub>2</sub> – PLA<sub>2</sub>) release, indicating that the relief without PLA<sub>2</sub> was significantly lower (40% without PLA<sub>2</sub> vs 90% with of PLA<sub>2</sub> after 24 h). Then, Pang *et al.* proceeded to investigate the antibacterial effect of liposome-loaded **12**. At 20 μM concentration **12** enclosed in the liposomes had poor antibacterial activity when combined with US (1.3 log reduction of MRSA and 0.52 log for *E. coli ESBL +*). Liposomes unmodified by maltohexaose moiety, unloaded **12** and unloaded liposomes did not show any significant activity, as well as liposomes with the addition of PLA<sub>2</sub> inhibitor. Additionally, none of the mentioned substances had any effect without US irradiation. Pang *et al.* investigated also the influence of **12** nanoliposomes concentration, which varied from 5 to 20 μM, showing that higher concentration of the nanoliposomes had slightly better antibacterial effect, up to approx. 95% (1.3 log) for MRSA and approx. 70% (0.5 log) for *E. coli ESBL +*.<sup>[35]</sup> Bridging the SS with other supporting molecules can be beneficial, especially when these molecules act in a similar way to enzymes, thus being called nanozymes. An example of nanozyme-bridged porphyrin was provided by Sun *et al.* in 2020 tetrakis(4-carboxyphenyl)porphyrin **13** (TCPP, Figure 6), bonded with nanoplates of palladium inlaid with platinum against MRSA.<sup>[75]</sup> The nanoplates were equipped with functional groups delivered by modified poly(ethylene glycol) (PEG), with a thiol group on one side of the chain and the amine group on the other. This allowed to bond **13** to

nanoplates through the amide bond. Sun *et al.* determined firstly the catalytic activity of palladium-platine nanoplates bonded with **13**, as well as the nanoplates alone, in hydrogen peroxide decomposition. The investigation was led for up to 450 s without irradiation, showing that the nanoplates without the porphyrin moiety could produce molecular oxygen, giving approximately 20 mg/L of O<sub>2</sub>. Otherwise, the nanoplates having a porphyrin moiety had no significant effect on molecular oxygen production, thus the investigation was repeated with irradiation at 1 MHz frequency and 0.97 W/cm<sup>2</sup> power density in 50% duty cycle, resulting in the production of approx. 22 mg/L of oxygen. What is more, the irradiation also resulted in a more rapid reach of maximum production than for nanoplates having neither porphyrin moiety nor US irradiation. Additionally, the US alone also had an effect in increasing the rate of hydrogen peroxide decomposition, although it was insignificant (approx. 2.5 mg/L compared to approx. 1 mg/L without irradiation). Having determined the generation of oxygen, Sun *et al.* also investigated the generation of singlet oxygen by the **13**-enhanced nanoplates, measured as changes in fluorescence of dichlorofluorescein diacetate (DCFH-DA). The study without additional hydrogen peroxide shows, that under 3 min irradiation the generation of singlet oxygen was high, while without the US it was insignificant. Moreover, the addition of hydrogen peroxide elevated ROS production even more. The next step was determining the antibacterial efficiency of porphyrin-enhanced nanoplates. The study indicated that 50 ppm of the nanoplates had a significant antibacterial effect, nearly 100% in the presence of US (after 8 min of irradiation). Without nanoplates, the effect was much lower, approximately 30% (0.15 log). These results were compared to **13** alone, and nanoplates without **13** moieties, having an effect of nearly 60% (0.22 log) and around 50% (0.3 log), respectively when irradiated. Both had no significant antibacterial effect while not irradiated with US.<sup>[75]</sup> A similar approach of SS modification with metals with catalytic properties was examined by Yu *et al.*<sup>[67]</sup> The porphyrin SS – **13** was not bonded with metal particles, but chelated the metal (Pt) ions. A new designed SS was tested against MRSA of *S. aureus*. The compound was a cube-shaped cluster of porphyrin rings obtained from the reaction with zirconium chloride, which was then used as chelating agents for platinum coming from hexachloroplatinic acid. The chelated clusters had then nanorods of gold loaded on the surface. Yu *et al.* investigated the yield of singlet oxygen generation by obtained systems, as changes in DPBF fluorescence. The parameters of US were 1 MHz frequency, the power density of 1.5 W/cm<sup>2</sup> with 50% duty cycle, and time up to 100 s. It was noticed that the porphyrin cluster alone had no significant impact on DPBF fluorescence, thus its activity in the production of singlet oxygen was negligible. However, the ones merged with platinum and those combined also with gold nanorods showed significant production of singlet oxygen, slightly higher for the gold-associated ones. The fluorescence of DPBF changed over time, for the first 20 seconds rapidly, reaching approx. 40% decrease for SS not associated with gold and approx. 47% while gold nanorods were present in its structure. Then the fluorescence diminished rather slowly, but still, reaching approx.

50% decrease while gold was not present, up to 70% when gold nanorods were associated with the cluster. The next part of the study was the determination of antibacterial activity of developed systems (400  $\mu\text{g}/\text{mL}$ ) after 15 min of US irradiation. All three systems were compared to US treatment alone which as well as porphyrin cluster not chelating the platinum atoms had activity of 34.14% (0.18 log), the one chelating the platinum and not associated with gold particles had an activity of 97.86% (1.67 log) while the association with gold had an effect of 99.93% (3.15 log).<sup>[67]</sup> Not only metal in atomic form can be successfully associated with SS, as shown by Wang *et al.*, who bonded titanium dioxide, being SS itself, with sinoporphyrin sodium **14** (DVDMS, Figure 6) and investigated its activity against *S. aureus*.<sup>[65]</sup> The compound was obtained by dissolving **14** in saline dispersion of  $\text{TiO}_2$  modified with Pluronic F127 (a tri-block polymer of poly(ethylene glycol) and poly(propylene glycol)). Next, the efficiency of the obtained compound in the production of ROS, especially hydroxyl radicals and singlet oxygen were evaluated, measured as changes in fluorescence of hydroxy terephthalic acid and singlet oxygen sensor green (SOSG), respectively. The yield of hydroxyl radicals formation was measured for  $\text{TiO}_2$  nanoparticles under 60 s irradiation at 1 MHz frequency and 3  $\text{W}/\text{cm}^2$  of power density, while the concentrations of  $\text{TiO}_2$  varied from 20 to 120  $\mu\text{g}/\text{mL}$ . This shows that the most efficient production of the radicals was at a concentration of 50  $\mu\text{g}/\text{mL}$ , thus this concentration was established as optimal and used for further studies. The singlet oxygen generation was investigated using the US with 1 MHz frequency and the power density varying from 1 to 5  $\text{W}/\text{cm}^2$  with or without the addition of  $\text{TiO}_2$ . After 60 s of irradiation, the best singlet oxygen formation yield for the US alone was observed with the highest power density. Interestingly, in the presence of  $\text{TiO}_2$ , the best yield of singlet oxygen generation in the whole system was observed at 3  $\text{W}/\text{cm}^2$ . Further studies of ROS generation were performed as the comparison between  $\text{TiO}_2$  nanoparticles and those modified with Pluronic F127, both in the concentration of 50  $\mu\text{g}/\text{mL}$  and with or without irradiation of 1 MHz frequency and 3  $\text{W}/\text{cm}^2$  of power density. The study shows that without US irradiation both  $\text{TiO}_2$  types had insignificant ROS generation. In contrast, the US alone presented a significant effect, elevated slightly by the addition of unmodified and F-127-modified  $\text{TiO}_2$  nanoparticles. Wang *et al.* determined the optimal concentration of **14**- $\text{TiO}_2$  for the generation of hydroxyl radicals. The irradiation was performed for 60 seconds and had still 1 MHz frequency and 3  $\text{W}/\text{cm}^2$  of power density, while the concentration varied from 10 to 160  $\mu\text{g}/\text{mL}$ . The obtained results led to the conclusion that 20  $\mu\text{g}/\text{mL}$  is an optimal one and was used in further steps. US alone had significant effect on hydroxyl radicals generation, elevated slightly when combined with **14**. Combination with  $\text{TiO}_2$  presented relatively higher effect, that increased insignificantly for **14**-modified  $\text{TiO}_2$ . Additionally, for generation of singlet oxygen, US alone had insignificant effect as well as combined with **14** and  $\text{TiO}_2$  respectively. In opposition, the combination of **14**- $\text{TiO}_2$  with US presented significant generation of singlet oxygen. Wang *et al.* have studied then the activity of DVDMS-modified  $\text{TiO}_2$  against *S. aureus*, with

concentration of  $\text{TiO}_2$  established at 40  $\mu\text{g}/\text{mL}$ . The activity of US alone and non-irradiated **14**- $\text{TiO}_2$  were visible, but did not differ significantly, revealing approx. 40% (0.22 log) and 50% (0.3 log) of activity, respectively, but when combined, the activity slightly elevated insignificantly, reaching 92.41% (1.12 log) of bacteria inactivation.<sup>[65]</sup>

### 3.4. To cure cancer

The US can be used for cancer therapy in sonodynamic and hyperthermic procedures. Hyperthermic cancer treatment involves high-intensity focused ultrasound, while SDT is based on the application of SS which is a chemical agent that after activation by the low-intensity US produces cytotoxic reactive oxygen species within a limited area of the tumor.<sup>[1]</sup> This approach is becoming more and more popular in cancer treatment. Recent studies aim to develop SSs that will be both insensitive to light to avoid the undesirable skin sensitivity occurring during PDT and able to improve tumor selectivity. SDT seems to be a promising tool for cancer patients with solid, even deep-located tumors due to increased depth of tissue penetration of US in comparison to regular PDT, minimally invasive properties, and application repeatability.<sup>[76,77]</sup> In the SDT procedure the US beam can be directed at the location of the tumor to avoid its distribution between the US source and the tumor tissue.<sup>[78]</sup> Low-intensity US does not affect the cell reproductive ability which is usually associated with hyperthermia after exposure to high intensity of US. Scientific reports on SDT do not specify side effects but describe them only as a minor.<sup>[79]</sup> According to Rengeng *et al.* and many studies investigating the issue of US of low frequency the modality improves the delivery of antitumor drugs by reversible opening the tight junction of blood vessel endothelium which means breaking the blood-tumor barrier.<sup>[80]</sup> Such parameters of SDT help to reduce damage to non-target sites and make this approach more favorable than PDT.<sup>[81,82]</sup> PDT patients feel pain during irradiation and after the procedure skin lesions (erythema, exudation, urticaria) and ocular adverse effects occur (acute severe visual acuity decrease). Other rarely observed side effects of PDT belong to scarring, altered hair growth, pigmentary change, and allergic reactions.<sup>[83–85]</sup>

SDT in cancer treatment:

- Is an alternative method to conventional chemotherapy, radiotherapy, and immunotherapy
- Is stimuli-responsive therapeutic approach alternative to PDT
- Employs ultrasounds to stimulate ROS generation
- Uses SSs to damage only cancer cells, not the healthy tissues
- Has high tissue penetration capability to reach deep-seated targets or large tumors
- Minimizes side effects in comparison to PDT.<sup>[86]</sup>

For SDT various types of SSs are tested (Table 2). There are mainly porphyrin-derivatives e.g. Photofrin, porphyrin, hematoporphyrin (Figure 7); xanthene derivatives, such as Rose bengal (Figure 5); curcumin, indocyanine green, acridine orange, hypocrellin B, (Figures 5 and 7) and antibacterial drug-based compounds (fluoroquinolones, Figure 5).<sup>[1]</sup> SSs should



Cancer type	SS and concentrations (calculated for drug)	US parameters	Duty cycle	Irradiation time [min]	Power density [J/cm <sup>2</sup> ]	Reduction	Ref.
Mouse sarcoma	Hp <b>15</b> (50 μM)	1.92 MHz, 3.18 W/cm <sup>2</sup>	100%	1 min	190.8	97.7%	[88]
Rat ascites hepatoma	ATX-70 <b>16</b> (2 μM/kg b.w.)	2 MHz, 5 W/cm <sup>2</sup>	100%	15 min	4500	75.5% <sup>[a]</sup>	[89]
Mouse colon-26 carcinoma	Photofrin II <b>17</b> (4 μM/kg b.w.)	1.92 MHz, 5 W/cm <sup>2</sup>	100%	15 min	4500	55% <sup>[a]</sup>	[90]
Breast cancer MDA-MB-231	<b>Porphyrin 18</b> @TiO <sub>2</sub> (0.028 μM)	20 MHz, 1 W/cm <sup>2</sup>	100%	1 min	60	47% <sup>[a]</sup>	[11]
Colon cancer HCT116	DVDMS <b>14</b> (4 μM)	0.97 MHz, 3.45 W	30%	3 min	[a]	28% <sup>[a]</sup>	[91]
Colon cancer RKO	DVDMS <b>14</b> (8.5 μM)	0.97 MHz, 0.32 W	30%	3 min	[a]	21% <sup>[a]</sup>	[92]
Human glioblastoma U87 MG	Microbubble- <b>RB 5</b> (0.54 mM)	1 MHz, 3 W/cm <sup>2</sup>	50%	3.5 min	315	287%	[93]
Mouse pancreatic cancer T110299	<b>Ce6 11</b> -CpG@ TiO <sub>2</sub> (9 μM)	1 MHz, 2 W/cm <sup>2</sup>	50%	4 min	240	83% <sup>[a]</sup>	[94]
Murine hepatoma	CM Dextran@ TiO <sub>2</sub> @MnO <sub>2</sub> - (0.4 mM)	[a], 10 W	20%	5 min	[a]	89% <sup>[a]</sup>	[95]
Mouse squamous cell carcinoma SCC7	<b>Hp 15</b> -poly(Glu-Tyr) (17 μM)	1 MHz, 3.5 W/cm <sup>2</sup>	50%	0.5 min 3.5 min	52.5 367.5	93% <sup>[b]</sup> 64%	[96]
Prostatic cancer	<b>TiO<sub>2</sub>/C</b> (0.1 mM) (41 mM)	1 MHz, 0.5 W/cm <sup>2</sup>	50%	1 min	15	50% <sup>[a,b]</sup> 82% <sup>[a]</sup>	[19]
Pancreatic cancer	<b>ICG 19</b> /Folic acid (26 μM) (129 μM)	1 MHz, 0.3 W/cm <sup>2</sup>	100%	1 min 3 min	18 54	57.65% <sup>[b]</sup> 94% <sup>[a]</sup>	[97]
Breast cancer MCF-7	<b>FA-HMME 10</b> -Melanin-PLGA (1.6 mM) (16 mM)	1 MHz, 1.5 W/cm <sup>2</sup>	100%	0.5 min	45	90% <sup>[a,b]</sup> 77% <sup>[a]</sup>	[98]
Human breast cancer MB-231							
Human lung cancer A-549							

[a] Exact data were not provided. [b] *in vitro*.

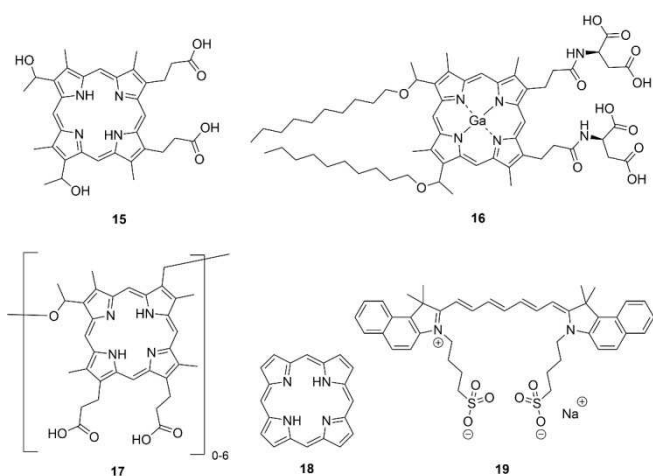


Figure 7. Structures of various porphyrinoid and non-porphyrinoid SSs.

exhibit good biocompatibility, high bioavailability and specificity, as well as excellent sonodynamic efficiency.<sup>[87]</sup> Moreover, various nanoparticle formulations have been designed lately. They include nanocarriers able to deposit SS selectively into tumor tissue with a simultaneous lack of systematic toxicity. Worth mentioning are microbubbles used as adjuvants for SSs and also enhancers of thermal effects able to disturb the tumor vasculature.

SDT has been developed since Yumita *et al.* started their research in the late eighties and then nineties of the 20th century.<sup>[88]</sup> They exposed cells of mouse sarcoma or cells of rat ascites hepatoma to the US (at three intensities: 1.27, 2.21, and 3.18 W/cm<sup>2</sup>) alone or in combination with hematoporphyrin 15 (Hp, Figure 7) at three concentrations: 10, 20, and 50 μg/mL for up to 60 s *in vitro*. They concluded that 15 alone did not enhance the cytotoxicity but increased the sensitivity of tumor cells to US. The US alone damaged 30 and 50% of tumor cells respectively, while in the presence of 15 97.7% and 95.5% of tumor cells were damaged respectively.<sup>[88]</sup> In further experiments, a gallium-porphyrin complex, ATX-70 16 (Figure 7), was tested on mice to indicate the potential of 16 to sensitize tumors to the US.<sup>[89]</sup> The animals were bearing colon-26 carcinoma tumor which was grown from colon-26 tumor model cell line and then transplanted to their bodies. Similarly, US (at the intensity of 3 W/cm<sup>2</sup>) alone revealed a slight antitumor effect, but it improved with the increased dose of 16 (2.5 mg/g b.w. or higher) indicating that the cytotoxic effect was related to sonochemical activation. A significant synergistic effect was recorded for 2.5 mg/kg b.w. or a higher dose of 16 and the three-field US intensity of 3 W/cm<sup>2</sup> or higher.<sup>[89]</sup> The next tests were directed at investigating the potential of Photofrin II 17 (PF, Figure 7) in SDT.<sup>[90]</sup> 17 turned out to be a good sensitizer of solid tumors to the US (at the intensity of 1, 2, 3, and 5 W/cm<sup>2</sup>) in mice bearing transplanted tumor colon 26 carcinomas. The highest concentration of 17 was measured 24 hours after the

**Table 3.** The efficiency of different combined sonodynamic and photodynamic approach in treating cancer and bacteria.

Cancer type or bacteria strain	Sensitizer and concentration	US parameters	Duty cycle	Light parameters	Irradiation time [min]	Reduction	Ref.
Breast cancer	SF1, Sfa, UF ( <sup>[a]</sup> $\mu\text{M}$ )	1 MHz, 2 W/cm <sup>2</sup>	75 %	554 nm, 45 mW/cm <sup>2</sup>	30 PDT + 20 SDT	<sup>[a]</sup>	[106]
Colon carcinoma CT26	ZnPc <b>20</b> (1.5 $\mu\text{M/kg}$ b.w.)	1.1 MHz, 1 W/cm <sup>2</sup>	100 %	670 nm, 160 mW/cm <sup>2</sup>	<sup>[a]</sup> PDT + 10 SDT	<sup>[a]</sup>	[107]
Murine mammary cancer 4T1	Ce6 <b>11</b> (1.7 $\mu\text{M}$ )	1 MHz, 0.36 W/cm <sup>2</sup>	100 %	650 nm, 1.04 mW/cm <sup>2</sup>	1 SDT + 2 PDT	52.2 %	[108]
Murine mammary cancer 4T2	Ce6 <b>11</b> (17 $\mu\text{M/kg}$ b.w.)	2 MHz, 0.36 W/cm <sup>2</sup>	100 %	650 nm, <sup>[a]</sup> W/cm <sup>2</sup>	1 SDT + <sup>[a]</sup> PDT <sup>[a]</sup> PDT + 1 SDT	52.17 % 55.7 %	[109]
Human breast cancer MDA-MB-231					1 SDT + <sup>[a]</sup> PDT <sup>[a]</sup> PDT + 1 SDT	55 % 48.8 %	
Human breast cancer MCF-7					1 SDT + <sup>[a]</sup> PDT <sup>[a]</sup> PDT + 1 SDT	44.34 % 53.62 %	
Prostate cancer LNCaP	Pheophorbide-a <b>21</b> (0.25 $\mu\text{M}$ )	1 MHz, 0.5 W/cm <sup>2</sup>	100 %	<sup>[a]</sup> nm, 0.5 mW/cm <sup>2</sup>	1 SDT + <sup>[a]</sup> PDT	98.34 %	[110]
Prostate cancer PC3						97 %	
Prostate cancer PC3	Bis (2-quinolinethiol) SiPc <b>22</b> (40 $\mu\text{M}$ ) Bis (8-quinolinoxy) SiPc <b>23</b> (40 $\mu\text{M}$ )	<sup>[a]</sup> MHz, 0.5 W	100 %	<sup>[a]</sup> nm, 0.5 mW	1 SDT + 1 PDT	90 % 95 %	[111]
Mouse mammary cancer 4T1	DVDMS <b>14</b> (0.5 $\mu\text{M}$ )	0.84 MHz, 0.25 W/cm <sup>2</sup>	100 %	635 nm, 23 mW/cm <sup>2</sup>	1 PDT + 1 SDT	85.01 % 86 %	[112]
Human breast cancer MDA-MB-231						77.48 %	
Human breast cancer MCF-7						19.11 %	[116]
Human gastric adenocarcinoma MKN-28	Tetrakis (cinnamyloxy) phthalocyanine <b>24</b> (10 $\mu\text{M}$ ) Gallium tetrakis (cinnamyloxy) phthalocyanine <b>25</b> (10 $\mu\text{M}$ ) Indium tetrakis (cinnamyloxy) phthalocyanine <b>26</b> (10 $\mu\text{M}$ )	1 MHz, 0.5 mW/cm <sup>2</sup>	100 %	600-800 nm, 0.5 mW/cm <sup>2</sup>	1 SDT + 1 PDT		
Liver cancer HEP G2	Curcumin <b>7</b> (2.5 mM/kg b.w.)	3 MHz, 2 W/cm <sup>2</sup>	60 %	445 nm, 500 mW	10 SDT + 6 PDT	45.4 %	[115]
Prostate cancer PC3	TiO <sub>2</sub> (10 $\mu\text{M}$ )	1 MHz, 0.5 W/cm <sup>2</sup>	100 %	<sup>[a]</sup> nm, 0.5 mW/cm <sup>2</sup>	1 SDT + <sup>[a]</sup> PDT	87.17 %	[117]
<i>S. aureus</i>	Curcumin <b>7</b> (80 $\mu\text{M}$ )	3 MHz, 3 W/cm <sup>2</sup>	50 %	460 nm, 37 mW/cm <sup>2</sup>	32 SDT + 32 PDT	3.48 log	[119]

[a] Exact data were not provided.

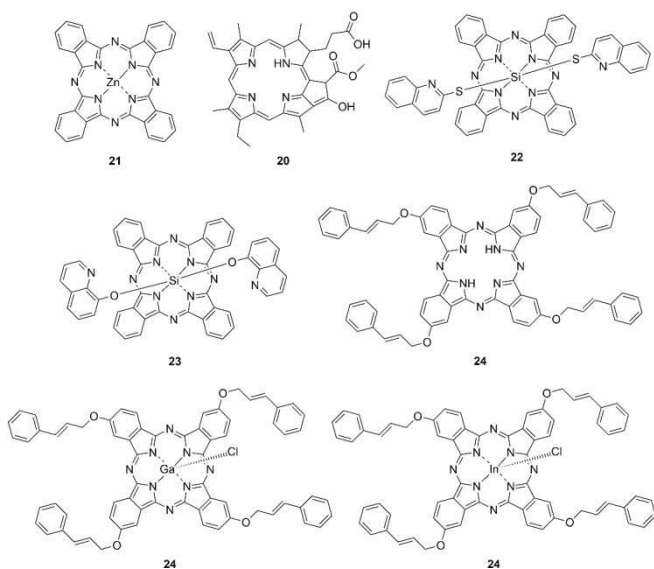


**Figure 8.** Structures of various porphyrinoid sensitizers used for combined PDT and SDT.

intravenous administration. Therefore, 24 hours after the intravenous administration was selected as the optimum timing for exposure to US. **17** used alone showed no significant effect, ultrasound applied alone showed a slight antitumor effect (at the three-field ultrasonic intensity of 3 and 5 W/cm<sup>2</sup>), while the effect increased significantly with the addition and rise of the dose of **17** proving a synergistic antitumor activity.<sup>[90]</sup> Nowadays the efficacy of SDT is often enhanced by the use of targeted delivery systems. Formulations based on nanoparticles enable the SSs to reach specifically the tumor site and accumulate there due to the enhanced permeability and retention (EPR) effect. Nanoparticles with nucleation sites generate bubbles that improve SDT effects.<sup>[87]</sup> Ansari and Eslami prepared TiO<sub>2</sub> nanoparticles from titanium tetraisopropoxide, hydrochloric acid 37%, and deionized water.<sup>[1]</sup> The surface of TiO<sub>2</sub> was modified with polyvinyl alcohol polymer and next with porphyrin **18**. The therapeutic effect of TiO<sub>2</sub> and the **18**-containing nanoparticles mediated SDT on breast cancer MDA-MB-231 cell lines was evaluated with MTT tests. US was applied at intensities of 1.0 W/cm<sup>2</sup> for 60 s in the presence and absence of TiO<sub>2</sub> nanoparticles functionalized with **18** (at concentrations of 0.01, 0.02 and 0.03  $\mu\text{g/mL}$ ). It turned out in the MTT tests that the nanoparticles were not harmful, but in the presence of

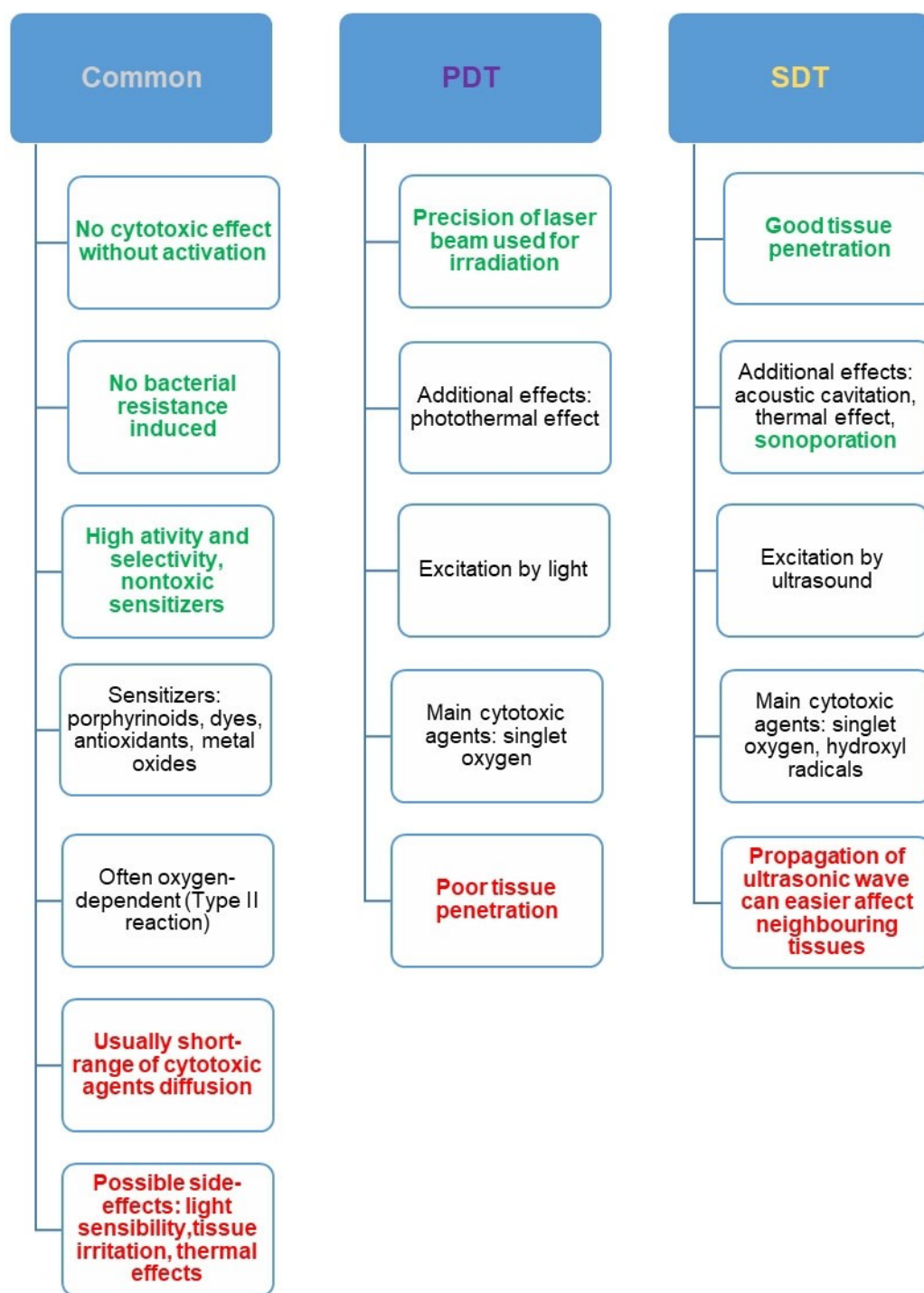


Figure 9. Main features, advances and drawbacks associated with PDT and SDT.

US radiation, they revealed toxic properties in killing breast cancer cells. Cell viability was investigated 1 h and 2 h after the first irradiation.<sup>[1]</sup> Shen *et al.* investigated SDT in combination with **14** in the treatment of two types of human colon cancer cells (HCT116 and RKO) *in vitro*.<sup>[91]</sup> The results were compared for a control group without any treatment, a group treated with **14**, a group treated with the US only, and a group treated with **14**-mediated SDT. The ultrasonic parameters were the follow-

ing: center frequency 0.970 MHz, acoustic power: 3.45 W, duration 3 min., duty cycle 30%. When the SS was activated by the US, it caused apoptosis, whereas intracellular ROS levels remarkably increased. **14** mediated SDT appeared to be the most effective approach against cancer cells.<sup>[91]</sup> Shen *et al.* continued their studies on the antitumor efficacy of SDT in combination with **14** on human glioblastoma (U87 MG) cell lines *in vitro*.<sup>[92]</sup> Cells were divided into four groups to undergo

different procedures: no treatment (control), **14** alone, US alone and **14** combined with SDT (center frequency: 0.970 MHz; peak-rarefactional pressure: 0.52 MPa; acoustic power: 0.32 W; pulse repetition frequency: 1 Hz; duty cycle: 1, 10 and 30%; duration 3 min). The incubation time and concentration of **14** were studied to monitor cellular uptake. For incubation time testing (0, 0.5, 1, 2, 3, 4 and 6 h) the concentration of **14** equal to 10  $\mu\text{g}/\text{mL}$  was chosen. After 24 h of incubation, various concentrations (1, 5, 10, and 20  $\mu\text{g}/\text{mL}$ ) of **14** were introduced into the culture medium and incubated for 3 h. It turned out that **14** easily entered the cancer-affected cells and accumulated mainly in the mitochondrial cytoplasm. Its intracellular concentration increased with incubation time or concentrations. Because of the application of SDT, ROS were remarkably generated, and mitochondrial membrane potential (MMP) was lost after 1 h post-treatment, indicating that the cytotoxic mechanism is associated with apoptosis. In the case of using **14** alone, no cytotoxicity was observed which confirmed the potential of **14**-mediated SDT in cancer treatment.<sup>[92]</sup> Nesbitt *et al.* investigated two advantages of SDT – killing cancer cells due to ROS generation and stimulation of the adaptive immune system in a pre-clinical model of pancreatic cancer.<sup>[93]</sup> The aim of the study was the generation of the abscopal effect of a T110299 mouse model of pancreatic cancer. It seems that stimulating the immune system may increase the occurrence of the so-called abscopal effect, i.e., the shrinkage of tumors distant from the original, irradiation target source. They prepared lipid microbubbles loaded with **5** ( $\text{O}_2\text{MB-5}$ ) and tested the potential of microbubble-mediated SDT to limit tumor growth. They observed the bilateral tumor mouse model of pancreatic cancer. The target tumor was treated with the US alone (3.0  $\text{W}/\text{cm}^2$ , 1 MHz, 50% duty cycle, 20 s) and with  $\text{O}_2\text{MB-5}$  mediated SDT. Then it was compared with the off-target untreated tumor. 287% decrease in tumor volume in untreated animals was demonstrated after 11 days following the initial treatment with SDT. Tumor size decreased more to 369% after the combination of SDT with a monoclonal antibody directed against programmed cell death-1 ligand 1 (aPD-L<sub>1</sub>), with immune checkpoint inhibitory (ICI) activity. In the analysis of tumor tissue elevated levels of CD4<sup>+</sup> and CD8<sup>+</sup> T-lymphocytes in the untreated tumors were found. SDT appeared to stimulate an adaptive immune response which was potentiated by the anti-PD-L<sub>1</sub> ICI.<sup>[93]</sup> Lin *et al.* also studied the possibility of applying SDT together with immunotherapy and nanoparticles.<sup>[94]</sup> They combined nanostructured titanium dioxide with **11**, and an immunological adjuvant CpG oligonucleotide (CpG ODN) to design a multifunctional formulation  $\text{TiO}_2\text{-11-CpG}$  whose anti-tumor efficacy was tested under US treatment. It turned out that the novel nano-SS inhibited tumor growth and additionally activated the adaptive immune response because of augmentation of SDT with  $\text{TiO}_2\text{-11}$  and enhancement of immune response with CpG. Mice were inoculated with tumors and divided into seven groups, including 1) phosphate-buffered saline (PBS), 2) US, 3)  $\text{TiO}_2\text{-CpG}$  + aPD-L1 + US 4)  $\text{TiO}_2\text{-11}$  + aPD-L1 + US 5)  $\text{TiO}_2\text{-11-CpG}$  + US 6)  $\text{TiO}_2\text{-11-CpG}$  + aPD-L1 7)  $\text{TiO}_2\text{-11-CpG}$  + aPD-L1 + US. After nine days the selected formulations were injected into tumors on the right flank of each mouse. On the tenth day,

some groups of animals were subjected to US irradiation (frequency 1.0 MHz, duty cycle 50%, power density 2.0  $\text{W}/\text{cm}^2$ , duration 7 min.) After applying blockade of aPD-L1 (at the dose of 50  $\mu\text{g}/\text{mouse}$ ), treatment of primary and metastatic tumors of liver cancer in mice with nano-SS under US led to promising results. Both the primary tumor growth and the non-irradiated pre-existing distant tumors were inhibited demonstrating the synergistic effect of the strategy. The generated systemic anticancer immunity concerned the activated maturation of dendritic cells and stimulation of cytotoxic CD8<sup>+</sup> T-lymphocytes. This approach offered a new perspective for treating malignant tumors.<sup>[94]</sup> Um *et al.* designed carboxymethyl-dextran nanocomposites for their potential use in the presence of SDT in anticancer treatment.<sup>[95]</sup> The formulation included  $\text{TiO}_2$ -based core as the SS,  $\text{MnO}_2$  coat as the chemosensitizer eliminating glutathione, the tumor growth-promoting agent, and the hydrophilic carboxymethyl-dextran shell. After the cellular uptake of the nanocomposites by the cancer cells, the drug formulation reduced  $\text{MnO}_2$  to  $\text{Mn}^{2+}$ , decreased intracellular GSH, and induced ROS generation. During application of US (power 10 W, duty cycle 20%, pulse repetition frequency 1 Hz, Y interval 2 mm) both the tested nanocomposite and the control nanocomposite (CNC, without  $\text{MnO}_2$ ) revealed cytotoxic activity. However, the tested formulation showed higher cytotoxicity than the control one. The nanocomposite mediated chemo-SDT leads to necrotic cell death and the release of HMGB1 antibodies stimulating further antitumor response.<sup>[95]</sup> Hadi *et al.* investigated the potential of a novel stimulus-responsive nanoparticle formulation in the treatment of prostate cancer.<sup>[96]</sup> They prepared the formulation based on the self-assembly of poly(L-glutamic acid-L-tyrosine) (PGATyr) copolymer with **15**. They tested the response of the formulation to a proteolytic enzyme cathepsin B secreted often in the solid tumor microenvironment and observed nanoparticle size reduction. The mice were divided into three groups depending on the treatment procedure. One group was subjected to **15**-carrying PGATyr-based nanoparticles. Two additional groups were treated either with the drug nanoformulation or with US irradiation and injection of PBS. Animals from the control group were treated with a PBS injection. In the presence of ultrasound cytotoxicity of the formulation increased against both applied human prostate cell lines LNCaP and PC3. In *in vivo* studies on SCID mice with ectopic human xenograft LNCaP tumors after systemic administration of a single dose of the nanoparticle formulation in the presence of US, tumor volumes were reduced up to 64% within 24 h. No adverse effects were observed in the animals and their body weight did not change. Such kind of approach seems to be promising in the treatment of prostate cancer and other recalcitrant cancers.<sup>[96]</sup> Cao *et al.* developed a novel formulation, a tablet-like  $\text{TiO}_2/\text{C}$  nanocomposite with a metal-organic-framework (MOF)-derived carbon structure to apply it to facilitate SDT under hypoxic conditions of solid pancreatic tumors.<sup>[19]</sup> They divided Panc02 cells into six groups, including 1) control 2) US 3)  $\text{TiO}_2/\text{C}$  4)  $\text{TiO}_2/\text{C}$  + US ( $\text{TiO}_2/\text{C}$  + US $\times$ 1) 5)  $\text{TiO}_2/\text{C}$  + US twice ( $\text{TiO}_2/\text{C}$  + US $\times$ 2) 6)  $\text{TiO}_2/\text{C}$  + US three times ( $\text{TiO}_2/\text{C}$  + US $\times$ 3). Cells were treated with  $\text{TiO}_2/\text{C}$  (equivalent Ti dose of 5  $\mu\text{g}/\text{mL}$ ) for 12 h and then



irradiated (0, 1, 2 or 3 times, 1 MHz, 0.5 W/cm<sup>2</sup>, duty rate 50%, 1 min.). Further cells were incubated for 12 h and subjected to cytotoxicity test (Cell Counting Kit – 8). Different equivalent Ti concentrations (0; 1.25; 2.5; 5 and 10 µg/mL) were applied to the cells for 12 h and later some cells were irradiated (in conditions mentioned before) or were left untreated and then apoptotic cell death was monitored. TiO<sub>2</sub>/C had no activity without US, however when irradiated, its cytotoxic effect increased along with concentration, reaching about 50% for 10 µg/mL equivalent Ti, either under normal or hypoxic conditions. *In vivo* studies were performed on mice separated into six groups, similarly to cell groups. Mice were inoculated with Panc02 cells inducing tumor growth and after 7 days treated with intravenous injection of PBS or TiO<sub>2</sub>/C (equivalent Ti concentration of 2 mg/mL). After 24 h mice were anesthetized and tumors were US irradiated an appropriate number of times (1 MHz, 0.5 W/cm<sup>2</sup>, duty rate 50%, 1 min). The treatment procedure was repeated on 0, 3, 6 days. After 14 days the animals were euthanized and tumors collected for tests. The novel formulation appeared to be hypoxia-tolerant, which is of great importance in the pancreatic tumor hypoxic microenvironment that limits the efficiency of oxygen-dependent type II SDT. Stability under US irradiation and generation of significant quantities of ROS under either normal or hypoxic conditions were advantages of the approach. Their yields were measured as changes in SOSG (for singlet oxygen), dihydrorhodamine (DHR, for superoxide radical) and aminophenylfluorescein (APF, for hydroxyl radical) fluorescence. However, for generation of hydrogen peroxide quantum yields were determined using H<sub>2</sub>O<sub>2</sub> assay kit and were about 0.03 mmol/L for equivalent Ti 40 µg/mL either under normal or hypoxic conditions. The nanocomposite not only led to DNA damage and tumor cell apoptosis but also revealed good biocompatibility and lack of apparent toxicity *in vivo* and *in vitro* representing a promising strategy for the treatment of hypoxic solid pancreatic tumors.<sup>[19]</sup> An interesting example of nanocarriers employed in formulation against breast cancer are exosomes (Exo) intended for use with SDT.<sup>[97]</sup> Exosomes conjugated with cancer-targeting ligand, folic acid (FA) were loaded with the SS, indocyanine green 19 (ICG, Figure 7). For such composition, aqueous stability and cellular uptake of 19 were improved, which led to increased ROS generation in cancer cells. US appeared useful for triggering the release of the 19 from exosomes as more 19 was released after their pretreatment with US (1 min., 0.3 W/cm<sup>2</sup>) which indicated US as a potential external stimulus for the release of 19 at the tumor site. It can be explained by the destabilization of the exosome membrane by the US. The influence of the US irradiation time (60, 70, 90 s) on the 19 releases from the FA-ExoICG was tested. Irradiation power was 0.3 W/cm<sup>2</sup>. It was observed that after longer irradiation more 19 was released from the formulation, which is beneficial for SDT efficiency. *In vitro* toxicity of 19-loaded exosomes was evaluated against folate receptor-negative hDFB and folate receptor-positive MCF-7 cells with MTT test. Cells were treated with 19 (20 µg/mL), Exo-19 (20 µg/mL 19, 3.55 · 10<sup>10</sup> exosomes/mL), FA-Exo-19 (20 µg/mL 19, 3.55 · 10<sup>10</sup> exosomes/mL) and irradiated (60 and 70 s). Irradiation turned out to be minimally cytotoxic to both

cell lines, whereas the cytotoxicity was particularly observed after irradiation combined with the application of Exo-19 or FA-Exo-19. In the case of *in vivo* studies, various samples (PBS, 19, Exo-19 and FA-Exo-19) were intravenously administered to MCF-7 tumor-bearing mice. The tumor sites were the US irradiated (3 min, 0.5 W/cm<sup>2</sup>) for 4 h or 24 h after administration. 14 days after US irradiation in mice subjected to the US and treated with Exo-19 or FA-Exo-19 tumor growth inhibition was remarkably demonstrated. The greatest reduction of tumor volume was observed for FA-Exo-19, which accumulated in tumors and revealed greater sonotoxicity to MCF-7 breast cancer cells than noncancerous human dermal fibroblast (hDFB) cells in comparison to free 19 or exosomes loaded with 19. Tumor growth in mice was inhibited after a single intravenous injection followed by US irradiation. In the study, the potential of the exosome - based nano-SSs together with SDT for the eradication of deep-seated tumors was confirmed.<sup>[97]</sup> Huang *et al.* developed folate receptor-targeted multifunctional formulation based on melanin nanoparticles and 10 (designed as FHMP NPs) for photoacoustic imaging-guided SDT with potential application for diagnostic-imaging and targeted therapeutic functionality (termed theranostics) in breast cancer.<sup>[98]</sup> Melanin nanoparticles (MNPs) were prepared due to their broad optical absorption expected from a contrast agent for photoacoustic imaging. Considering drawbacks of MNPs, such as quick heat diffusion upon photoacoustic (PA) laser irradiation and poor water solubility, poly (lactic-co-glycolic) acid (PLGA) was used as the biocompatible and biodegradable vehicle for the co-delivery of drugs. To improve the tumor-tissue penetration, folate receptor was chosen as the targeted entity with specific tumor sites selectivity. MDA-MB-231 human breast cancer cell line and A-549 human lung cancer cell line were employed into the studies. For the *in vitro* cytotoxicity evaluation, the cells were divided into six groups including the control group, the group subjected to US, the group treated with FMP NPs + US, the group treated with FHMP NPs, the group treated with HMP NPs + US and the group treated with FHMP NPs + US. After removing the culture medium different NPs (FA-MNP-PLGA NPs, 10-PLGA-FA NPs and FHMP NPs) were dispersed in RPMI-1640 medium at a concentration of 0.75 mg/mL or 1 mg/mL. After 3-hour incubation they were subjected to US irradiation at the intensity of 1.5 W/cm<sup>2</sup>, frequency of 1 MHz and duration of 30 s. *In vivo* tests were carried out on mice. The animals were injected with MDA-MB-231 cells in PBS solution to induce tumor growth. When the tumor volume reached 0.8 cm<sup>3</sup>, the mice were divided into five groups including: control, US, FMP NPs + US, FHMP NPs, FHMP NPs + US. The animals were injected 200 µL of different NPs for 3 h and subjected to US irradiation (3 W/cm<sup>2</sup>, 1 MHz, 5 min.). In the novel formulation better light stability of 10 was observed, improving sonodynamic performance and delivery of MNPs to the cancer tissue. Selective killing effect of ROS on tumor cells was investigated and confirmed.<sup>[98]</sup>

#### 4. Combination of Two Methods (SDT + PDT)

There are many obvious benefits of PDT that have been extensively described in numerous publications (Table 3). First, modern PDT is safe, minimally invasive, cheap, universal, effective even after a single application, can be combined with pharmacotherapy, and does not induce bacterial resistance or drug resistance. SDT is younger, but also getting attention.<sup>[4,10,99–101]</sup> Both treatments, as already mentioned, show important common elements. They require the presence of oxygen in the environment, a suitably selected active substance, and a (respectively) light or sound wave.<sup>[102]</sup> Unfortunately, each of these therapies has its highlights and limitations. The permeability of light wave through human tissues is very limited and additionally depends on the wavelength. On the other hand, the human body should not be exposed to the US for a long time due to its potentially harmful systemic effects.<sup>[103]</sup> So the natural question arises, is it possible to use the advantages of both therapies and limit their side effects? The answer to this question seems to be the relatively newly developed sono-photodynamic therapy (SPDT) or photo-sonodynamic therapy (PSDT), distinguished by the order of particular treatments.<sup>[102]</sup> Many studies show a better ability to generate ROS due to the complementary properties of both methods.<sup>[103–105]</sup> Moreover, the activity of US increases the permeability of cells, which simultaneously induces the apoptotic mechanism and leads to better penetration of the active substance.<sup>[102]</sup> In summary, with synergistic effects of US and light, SPDT may be an interesting, still under-researched area of minimally invasive therapy, especially new in the field of microbiology.

Zhang *et al.* have investigated a new systemic tumor therapeutic procedure called Sono Photo Dynamic Therapy (SPDT) in patients with advanced refractory breast cancer treatment, including metastases in the viscera, brain, and bones.<sup>[106]</sup> The PSs and SSs were given to patients sublingually. PDT treatment included irradiation with red LED light at 45 mW/cm<sup>2</sup> and 554 nm of wavelength for 30 min and it was followed by SDT treatment involving exposing the tumor area for 20 min at 1 MHz and 2.0 W/cm<sup>2</sup> or the whole body and tumor area for 40 min at 75% pulse, 1 MHz and 2.0 W/cm<sup>2</sup>. Some patients had concurrent chemotherapy. Despite the low number of participants (32 patients) in this study SPDT applied alone or in combination with chemotherapy seems to be a useful approach to reduce the tumor mass and prolong survival.<sup>[106]</sup> Another study confirmed the high efficacy of combining PDT with SDT in the treatment of induced colorectal cancer in a mouse model.<sup>[107]</sup> A liposomal formulation of zinc phthalocyanine **20** (ZnPc, Figure 8) was used by Bakhshizadeh *et al.* as PS. The results of single therapy (PDT, SDT) and combination therapy were compared and the obtained data were evaluated. After the 120-day follow-up, tumor regression was observed in each study group. Optimal results were obtained with SPDT dominated by PDT. SPDT with a dominant SDT showed significantly worse results. The authors suggest that this could be caused by the formation of pores in the tumor cells caused by SDT. The PS can potentially “leak” through the pores and therefore cannot

be active during exposure to light. It should be emphasized, that the authors did not investigate the relationship between the concentration and irradiation conditions and the effectiveness of the procedure. Only one parameter was used – US irradiation was performed in continuous mode with a frequency of 1.1 MHz and intensity of 1 W/cm<sup>2</sup> for 10 min.<sup>[107]</sup> Li *et al.* in their research came to different conclusions and indicated that the use of US by increasing the permeability of the membrane and the formation of pores enhances the penetration of the PS into the tumor cells.<sup>[108]</sup> They observed an increased accumulation of **11** in the mitochondria after 4 hours of incubation. Researchers applied ultrasound at 1.0 MHz for up to 1 min with an intensity of 0.36 W/cm<sup>2</sup> and then immediately laser light with a total radiation dose of 1.2 J/cm<sup>2</sup>. The combination of PDT and SDT gave very promising results – cell DNA damage, reduction of clonogenicity, and decreased cell viability were noted. It was indicated that these processes may be related to ROS activity and caspase activity. The use of N-acetylcysteine (ROS scavenger) and the caspase inhibitor z-VAD-fmk severely limited the therapeutic effect of the procedure.<sup>[108]</sup> Similar results with the use of **11** against breast cancer (MDA-MB-231, MCF-7, and 4T1 cell lines) were obtained by Wang *et al.* Also, significantly higher loss of viability of cells subjected to mixed therapy and increased production of ROS were observed. Interestingly, research has shown a significantly reduced level of VEGF and MMP-9 expression, which may play a key role in therapy.<sup>[109]</sup> Aksel *et al.* also studied strategies for the treatment of prostate cancer on androgen-sensitive (LNCaP) and androgen-insensitive cell lines (PC3).<sup>[110]</sup> They tried to compare the efficiency of Pheophorbide-a-mediated PDT, SDT, and SPDT therapies. The cells were incubated with different concentrations of Pheophorbide-a **21** (Figure 8), a porphyrin derivative of high photodynamic efficiency. Further cells were treated with 0.5 W/cm<sup>2</sup> of US and/or irradiated with a light dose of 0.5 mJ/cm<sup>2</sup>. The SPDT turned out to be the most effective in the inhibition of cell proliferation in comparison to both monotherapies. As a result of treatment, apoptosis was induced and an increase in the oxidative stress markers was observed.<sup>[110]</sup> Promising results of the combination of PDT and SDT have been also shown in studies on the effectiveness of therapy against prostate cancer.<sup>[111]</sup> Cells of the PC3 line were used analogously to the previously discussed experiment. Di-axially substituted silicon phthalocyanines **22** and **23** (Figure 8) at different concentrations were used as PS and their effects in PDT, SDT, and SPDT therapies were compared. Concentrations ranging from 2 to 40 μM were used and a positive correlation between concentration and efficacy in both PDT, SDT, and SPDT was observed. The analysis using the MTT method showed the maximum effect in the case of the combination of PDT and SDT, where a maximum of 95% reduction in cell viability was achieved.<sup>[111]</sup> Interesting results were obtained from a study comparing the efficacy of SPDT *in vivo* and *in vitro* breast cancer models.<sup>[112]</sup> The experiment used **10**, which is a newly developed PS. *In vivo* study proved that the use of SPDT significantly reduced the tumor volume and decreased the likelihood of metastasis. This study has confirmed the observations of other authors so far that the combination therapy

causes a marked increase in ROS compared to monotherapy. Using the terephthalic acid (TA) method and FD500-uptake assay, the increase in membrane permeability was confirmed. There was also a subtle difference between SPDT and PSDT in favor of PSDT, which corresponds to the results of Bakhshizadeh *et al.*<sup>[112]</sup> An interesting extension of SDT and PDT is the support of the active substance with modern carriers.<sup>[113]</sup> In recent years, there has been an intensive development of formulations that have been successfully used in PDT.<sup>[99,114]</sup> Currently, it is possible to extend their use from SPDT. A promising example was the combination of the innovative microbubble-mediated SPDT technology in combination with **7** and PLGA. The formulation was successfully used against HepG2 liver cancer cells. The formulation used showed good biocompatibility and the neutrality of the non-excited particles toward human cells. Microscopic analysis (nude mice) indicates that pyroptosis (caspase-mediated inflammatory cell death, occurring mostly as an effect of infection) and apoptosis were important and primary cell death mechanisms for cancer. These studies once again confirm the lethal mechanism based on the high concentration of ROS and the mitochondrial membrane potential loss. In another study, the same research group extended the experiment to glypican-3-targeted, **7**-loaded microbubbles used against HepG2 liver cancer cells.<sup>[115]</sup> The results correlated with the previous ones were obtained and SPDT turned out to be more effective than PDT or SDT alone. Similar conclusions were drawn by Güzel *et al.*, who tested novel metal-free **24**, gallium **25**, and indium **26** phthalocyanines with cinnamoyl moiety.<sup>[116]</sup> The phthalocyanines, especially **26** showed decent activity against MKN-28 adenocarcinoma cells when combined with SPDT, and also with SDT and PDT, but with lesser effect.<sup>[116]</sup> An interesting development of the SPDT technique was proposed by Aksel *et al.* using extremely popular in the pharmaceutical world nanoparticles of TiO<sub>2</sub>.<sup>[117]</sup> TiO<sub>2</sub> nanoparticles have been utilized as the basic active substance due to their photodynamic properties.<sup>[118]</sup> It was used against prostate cancer cells (PC3 cell line). The cells exposed to the PS were subjected to 0.5 W/cm<sup>2</sup> US and/or 0.5 W/cm<sup>2</sup> light irradiation. Also, in this case, the undoubted synergy of PDT and SDT was observed.<sup>[117]</sup> PDT has found an extremely wide application as a method of killing bacteria.<sup>[4,10]</sup> An interesting but poorly studied extension of PACT is its combination with SDT. Alves *et al.* used **7** in the fight against *S. aureus* biofilm. In the experiment, **7** was used at a dose of 80 μM, irradiated with a light dose of 70 J/cm<sup>2</sup> and US at 1 MHz and 3 W/cm<sup>2</sup>.<sup>[119]</sup> In each of the trials, better results were achieved with the use of SPDT, but the addition of sodium dodecyl sulfate (SDS) allowed for the almost complete killing of the bacteria.

## 5. Summary and Outlook

Photodynamic therapy, despite its many advantages and high efficacy, is limited by the excitation pathway. PSs start to work upon irradiation with visible light at wavelengths in the range of “phototherapeutic window”. Such kind of light can penetrate body tissues maximally up to 10 mm deep, depending on the

nature of the treated tissue. Developed light delivery systems improved this serious inconvenience also interstitial-PDT protocols have been designed. Nevertheless, such an approach does need an individualized light delivery system adjusted to the volume of solid tumors. On the other hand, photodynamic antimicrobial chemotherapy is much more effective against the planktonic form of bacteria in comparison to biofilms. The above drawbacks pushed scientists to try to overcome these problems. It was a pointed question: Can we use another excitation source? The solution to this problem seems to be the excitation of sensitizers with ultrasounds, commonly used in medicine. According to the overviewed reports they can be used to treat cancer cells as well as against bacteria. In Figure 9 crucial issues for PDT and SDT are listed.

In conclusion, modification of excitation source in PDT by introducing ultrasounds provides new perspectives and possibilities. It should be underlined that SDT for cancer treatment is not limited to superficial changes but opens up possibilities of curing cancer located inside the body. Nevertheless, in the case of bacteria inactivation, some protocols are ineffective. It can be caused by a lot of ultrasounds parameters in SDT in comparison to parameters of light in PDT. It has to be adjusted for acoustic power, repetition cycle of US, frequency, focusing of the waves, and many others. Taking all these aspects into consideration enables the treatment of deeply located tumors, not only solid ones. In the case of treating bacterial infections with SDT, it brings a big tool to combat bacteria in biofilm form, which is common in humans. Possibility of combining both methods should also be considered. Sono-photodynamic therapy (SPDT), a promising method using the combination of PDT and SDT, is highly advantageous in reducing the potential side effects compared to monotherapy. In addition, SPDT, which has become a crucial approach with the development of new potential sensitizers, will provide important alternative opportunities for the clinical cancer treatment and microbial diseases by using the synergistic effect of light and sound.

## Acknowledgements

Mr. Marcin Wysocki is a participant of STER Internationalisation of Doctoral Schools Programme from NAWA Polish National Agency for Academic Exchange No. PPI/STE/2020/1/00014/DEC/02. The research was financed from the small research grant from statutory funding for young researchers - doctoral students for 2022.

## Conflict of Interest

The authors declare no conflict of interest.

**Keywords:** Singlet oxygen · Porphyrinoids · Sensitizers · Cancer · Pathogens · Antitumor agents · Nanoparticles

- [1] E. Yousefi, S. Javadpour, M. Ansari, H. Eslami, *Mater. Technol.* **2021**, *36*, 521–528.
- [2] R. Zeeshan, Z. Mutahir, *Bosn J of Basic Med Sci* **2017**, *17*(3), 172–182.
- [3] D. C. S. Costa, M. C. Gomes, M. A. F. Faustino, M. G. P. M. S. Neves, A. Cunha, J. A. S. Cavaleiro, A. Almeida, J. P. C. Tomé, *Photochem. Photobiol. Sci.* **2012**, *11*, 1905.
- [4] L. Sobotta, P. Skupin-Mrugalska, J. Piskorz, J. Mielcarek, *Eur. J. Med. Chem.* **2019**, *175*, 72–106.
- [5] Y. Feng, C. Coradi Toton, S. Ashraf, T. Hasan, *Adv. Drug Delivery Rev.* **2021**, *177*, 113941.
- [6] W. C. Reygaert, *AIMS Microbiology* **2018**, *4*, 482–501.
- [7] D. Costley, H. Nesbitt, N. Ternan, J. Dooley, Y. Y. Huang, M. R. Hamblin, A. P. McHale, J. F. Callan, *Int. J. Antimicrob. Agents* **2017**, *49*, 31–36.
- [8] F. Harris, S. R. Dennison, D. A. Phoenix, *Trends Mol. Med.* **2014**, *20*, 363–367.
- [9] I. Yoon, J. Z. Li, Y. K. Shim, *Clin Endosc* **2013**, *46*, 7.
- [10] L. Sobotta, P. Skupin-Mrugalska, J. Piskorz, J. Mielcarek, *Dyes Pigm.* **2019**, *163*, 337–355.
- [11] J. M. Dąbrowski, L. G. Arnaut, *Photochem. Photobiol. Sci.* **2015**, *14*, 1765–1780.
- [12] P. Agostinis, K. Berg, K. A. Cengel, T. H. Foster, A. W. Girotti, S. O. Gollnick, S. M. Hahn, M. R. Hamblin, A. Juzeniene, D. Kessel, M. Korbelik, J. Moan, P. Mroz, D. Nowis, J. Piette, B. C. Wilson, J. Golab, *Ca-Cancer J. Clin.* **2011**, *61*, 250–281.
- [13] L. B. Josefsen, R. W. Boyle, *Met.-Based Drugs* **2008**, *2008*, 1–23.
- [14] P. R. Ogilby, *Chem. Soc. Rev.* **2010**, *39*, 3181.
- [15] B. Yang, Y. Chen, J. Shi, *Chem. Rev.* **2019**, *119*, 4881–4985.
- [16] J. M. Dąbrowski, in *Adv. Inorg. Chem.*, Elsevier, **2017**, pp. 343–394.
- [17] H. Abrahamse, M. R. Hamblin, *Biochem. J.* **2016**, *473*, 347–364.
- [18] L. Larue, B. Myrzakhmetov, A. Ben-Mihoub, A. Moussaron, N. Thomas, P. Arnoux, F. Baros, R. Vanderesse, S. Acherar, C. Frochot, *Pharmaceuticals* **2019**, *12*, 163.
- [19] J. Cao, Y. Sun, C. Zhang, X. Wang, Y. Zeng, T. Zhang, P. Huang, *Acta Biomater.* **2021**, *129*, 269–279.
- [20] R. R. Allison, K. Moghissi, *Clin Endosc* **2013**, *46*, 24.
- [21] F. Setaro, J. W. H. Wennink, P. I. Mäkinen, L. Holappa, P. N. Trohopoulos, S. Ylä-Herttuala, C. F. van Nostrum, A. de la Escosura, T. Torres, *J. Mater. Chem. B* **2020**, *8*, 282–289.
- [22] M. S. Gualdesi, J. Vara, V. Aiassa, C. I. Alvarez Igarzabal, C. S. Ortiz, *Dyes Pigm.* **2021**, *184*, 108856.
- [23] H. Kataoka, H. Nishie, N. Hayashi, M. Tanaka, A. Nomoto, S. Yano, T. Joh, *Ann Transl Med* **2017**, *5*, 183–183.
- [24] F. Nakonechny, M. Nisnevitch, Y. Nitzan, M. Nisnevitch, *BioMed Res. Int.* **2013**, *2013*.
- [25] M. Stolarska, A. Glowacka-Sobotta, D. T. Mlynarczyk, J. Długaszewska, T. Goslinski, J. Mielcarek, L. Sobotta, *Int. J. Mol. Sci.* **2020**, *21*, 6145.
- [26] G. A. Meerovich, E. V. Akhlyustina, I. G. Tiganova, E. A. Lukyanets, E. A. Makarova, E. R. Tolordava, O. A. Yuzhakova, I. D. Romanishkin, N. I. Philipova, Yu. S. Zhizhimova, Yu. M. Romanova, V. B. Loschenov, A. L. Gintsburg, in *Adv. Microbiol. Infect. Dis. Public Health* (Ed.: G. Donelli), Springer International Publishing, Cham, **2019**, pp. 1–19.
- [27] M. Thomas, J. D. Craik, A. Tovmasyan, I. Batinic-Haberle, L. T. Benov, *Future Microbiol.* **2015**, *10*, 709–724.
- [28] F. Le Guern, T.-S. Ouk, I. Yerzhan, Y. Nurlykyz, P. Arnoux, C. Frochot, S. Leroy-Lhez, V. Sol, *Molecules* **2021**, *26*, 1122.
- [29] W. Liao, X. Shi, L. Zhuo, X. Yang, P. Zhao, W. Kan, G. Wang, H. Wei, Y. Yang, Z. Zhou, J. Wang, *ACS Appl. Mater. Interfaces* **2021**, *13*, 41012–41020.
- [30] D. Ziental, J. Zajac, K. Lewandowski, J. Długaszewska, M. J. Potrzebowski, L. Sobotta, *Dyes Pigm.* **2022**, *201*, 110240.
- [31] B. Liu, D. J. Wang, B. M. Liu, X. Wang, L. L. He, J. Wang, S. K. Xu, *Ultrason. Sonochem.* **2011**, *18*, 1052–1056.
- [32] Y. Dong, H. Su, H. Jiang, H. Zheng, Y. Du, J. Wu, D. Li, *Ultrason. Sonochem.* **2017**, *37*, 1–8.
- [33] N. Kashaf, Y.-Y. Huang, M. R. Hamblin, *Nat. Photonics* **2017**, *6*, 853–879.
- [34] E. Polat, K. Kang, *Biomedicine* **2021**, *9*, 584.
- [35] X. Pang, Q. Xiao, Y. Cheng, E. Ren, L. Lian, Y. Zhang, H. Gao, X. Wang, W. Leung, X. Chen, G. Liu, C. Xu, *ACS Nano* **2019**, *13*, 2427–2438.
- [36] A. Pinto, Y. Mace, F. Drouet, E. Bony, R. Boidot, N. Draoui, I. Lobysheva, C. Corbet, F. Polet, R. Martherus, Q. Deraedt, J. Rodríguez, C. Lamy, O. Schicke, D. Delvaux, C. Louis, R. Kiss, A. V. Kriegesheim, C. Dessy, B. Elias, J. Quetin-Leclercq, O. Riant, O. Feron, *Oncogene* **2016**, *35*, 3976–3985.
- [37] D. Bechet, P. Couleaud, C. Frochot, M.-L. Viriot, F. Guillemin, M. Barberi-Heyob, *Trends Biotechnol.* **2008**, *26*, 612–621.
- [38] J. Tian, B. Huang, M. H. Nawaz, W. Zhang, *Coord. Chem. Rev.* **2020**, *420*, 213410.
- [39] D. Ziental, B. Czarczynska-Goslinska, D. T. Mlynarczyk, A. Glowacka-Sobotta, B. Stanisz, T. Goslinski, L. Sobotta, *Nanomaterials* **2020**, *10*, 387.
- [40] Y. Ju, X. Shi, S. Xu, X. Ma, R. Wei, H. Hou, C. Chu, D. Sun, G. Liu, Y. Tan, *Adv. Sci.* DOI: 10.1002/advsc.202105034.
- [41] S. Yang, X. Wang, P. He, A. Xu, G. Wang, J. Duan, Y. Shi, G. Ding, *Small* **2021**, *17*, 2004867.
- [42] M. Guan, Y. Zhou, S. Liu, D. Chen, J. Ge, R. Deng, X. Li, T. Yu, H. Xu, D. Sun, J. Zhao, T. Zou, C. Wang, C. Shu, *Biomaterials* **2019**, *213*, 119218.
- [43] A. C. S. Lobo, L. C. Gomes-da-Silva, P. Rodrigues-Santos, A. Cabrita, M. Santos-Rosa, L. G. Arnaut, *J. Clin. Med.* **2019**, *9*, 104.
- [44] N. W. Nkune, N. W. N. Simelane, H. Montaseri, H. Abrahamse, *Int. J. Mol. Sci.* **2021**, *22*, 12618.
- [45] X. Yu, H. Zheng, M. T. V. Chan, W. K. K. Wu, *Environ. Sci. Pollut. Res. Int.* **2018**, *25*, 20569–20574.
- [46] S. M. Gallagher-Colombo, A. L. Maas, M. Yuan, T. M. Busch, *Isr. J. Chem.* **2012**, *52*, 681–690.
- [47] R. L. G. Lecaros, L. Huang, T.-C. Lee, Y.-C. Hsu, *Mol. Ther.* **2016**, *24*, 106–116.
- [48] U. Schmidt-Erfurth, U. Schlotzter-Schrehard, C. Cursiefen, S. Michels, A. Beckendorf, G. O. H. Naumann, *Invest Ophthalmol Vis Sci* **2003**, *44*, 4473.
- [49] Y. Dong, G. Wan, P. Yan, Y. Chen, W. Wang, G. Peng, *Exp. Ther. Med.* **2016**, *12*, 3923–3926.
- [50] M. Suzuki, Y. Ozawa, S. Kubota, M. Hirasawa, S. Miyake, K. Noda, K. Tsubota, K. Kadonosono, S. Ishida, *J. Neuroinflammation* **2011**, *8*, 176.
- [51] X. Ma, H. Pan, G. Wu, Z. Yang, J. Yi, *Med. Hypotheses* **2009**, *73*, 18–19.
- [52] X. Wang, M. Ip, A. W. Leung, C. Xu, *Ultrasonics* **2014**, *54*, 2109–2114.
- [53] X. Wang, X. Zhong, L. Bai, J. Xu, F. Gong, Z. Dong, Z. Yang, Z. Zeng, Z. Liu, L. Cheng, *J. Am. Chem. Soc.* **2020**, *142*, 6527–6537.
- [54] C. Li, X. Q. Yang, J. An, K. Cheng, X. L. Hou, X. S. Zhang, Y. G. Hu, B. Liu, Y. Di Zhao, *Theranostics* **2020**, *10*, 867.
- [55] X. Zhong, X. Wang, L. Cheng, an Tang, G. Zhan, F. Gong, R. Zhang, J. Hu, Z. Liu, X. Yang, X. Zhong, G. Zhan, J. Hu, X. Yang, X. Wang, L. Cheng, F. Gong, R. Zhang, Z. Liu, Y. Tang, *Adv. Funct. Mater.* **2020**, *30*, 1907954.
- [56] D. Zhuang, C. Hou, L. Bi, J. Han, Y. Hao, W. Cao, Q. Zhou, *FEMS Microbiol. Lett.* **2014**, *361*, 174–180.
- [57] H. Chen, X. Zhou, Y. Gao, B. Zheng, F. Tang, J. Huang, *Drug Discovery Today* **2014**, *19*, 502–509.
- [58] J. Dai, M. Bai, C. Li, H. Cui, L. Lin, *Trends Food Sci. Technol.* **2020**, *105*, 211–222.
- [59] B. Duan, X. Shao, Y. Han, Y. Li, Y. Zhao, *J. Cleaner Prod.* **2021**, *290*, 125750.
- [60] C. Xu, J. Dong, M. Ip, X. Wang, A. W. Leung, *Ultrasonics* **2016**, *64*, 54–57.
- [61] M. Trendowski, *Cancer Metastasis Rev.* **2014**, *33*, 143–160.
- [62] M. Pourhajibagher, B. Rahmiesboei, M. Hodjat, A. Bahador, *Photodiagn. Photodyn. Ther.* **2020**, *30*, 101780.
- [63] C. Nguyen Huu, R. Rai, X. Yang, R. V. Tikekar, N. Nitin, *Ultrason. Sonochem.* **2021**, *74*, 105567.
- [64] Y. Zhang, H. Zhang, D. Zhuang, L. Bi, Z. Hu, W. Cao, *Microb. Pathog.* **2020**, *144*, 104192.
- [65] Y. Wang, Y. Sun, S. Liu, L. Zhi, X. Wang, *Ultrason. Sonochem.* **2020**, *63*, 104968.
- [66] L. Serpe, F. Giuntini, *J. Photochem. Photobiol. B* **2015**, *150*, 44–49.
- [67] Y. Yu, L. Tan, Z. Li, X. Liu, Y. Zheng, X. Feng, Y. Liang, Z. Cui, S. Zhu, S. Wu, *ACS Nano* **2021**, *15*, 10628–10639.
- [68] J. Guo, Y. Xu, M. Liu, J. Yu, H. Yang, W. Lei, C. Huang, *J. Mater. Chem. B* **2021**, *9*, 7686–7697.
- [69] M. Pourhajibagher, A. Bahador, *Photodiagn. Photodyn. Ther.* **2021**, *35*, 102432.
- [70] X. Wang, A. W. Leung, H. Hua, C. Xu, M. Ip, *J. Acoust. Soc. Am.* **2015**, *138*, 2548–2553.
- [71] X. Wang, M. Ip, A. W. Leung, Z. Yang, P. Wang, B. Zhang, S. Ip, C. Xu, *Ultrasonics* **2015**, *62*, 75–79.
- [72] X. Wang, M. Ip, A. W. Leung, P. Wang, H. Zhang, H. Hua, C. Xu, *Ultrasonics* **2016**, *65*, 137–144.
- [73] Heather L. Dolan, Luis J. Bastarrachea, Rohan V. Tikekar, *LWT* **2018**, *88*, 146–151.
- [74] D. Zhuang, J. Han, L. Bi, Y. Wang, Y. Hao, Q. Zhou, W. Cao, *Drug Des Devel Ther* **2015**, *9*, 2545–2551.
- [75] D. Sun, X. Pang, Y. Cheng, J. Ming, S. Xiang, C. Zhang, P. Lv, C. Chu, X. Chen, G. Liu, N. Zheng, *ACS Nano* **2020**, *14*, 2063–2076.



- [76] H. Shibaguchi, H. Tsuru, M. Kuroki, M. Kuroki, *Anticancer Res.* **2011**, *31*, 2425–2430.
- [77] D. Costley, C. McEwan, C. Fowley, A. P. McHale, J. Atchison, N. Nomikou, J. F. Callan, *Int. J. Hyperthermia* **2015**, *31*, 107–117.
- [78] H. Hirschberg, S. J. Madsen, *Ther. Delivery* **2017**, *8*, 331–342.
- [79] M. A. Hanson, *Health effects of exposure to ultrasound and infrasound: report of the independent advisory group on non-ionising radiation*, Health Protection Agency, Chilton, GB **2010**.
- [80] L. Rengeng, Z. Qianyu, L. Yuehong, P. Zhongzhong, L. Libo, *Photodiagn. Photodyn. Ther.* **2017**, *19*, 159–166.
- [81] L. Fan, Y. Liu, H. Ying, Y. Xue, Z. Zhang, P. Wang, L. Liu, H. Zhang, *J. Mol. Neurosci.* **2011**, *43*, 541–548.
- [82] X. Shang, P. Wang, Y. Liu, Z. Zhang, Y. Xue, *J. Mol. Neurosci.* **2011**, *43*, 364–369.
- [83] G. Gunaydin, M. E. Gedik, S. Ayan, *Front. Chem.* **2021**, *9*, 691697.
- [84] S. H. Ibbotson, T. H. Wong, C. A. Morton, N. J. Collier, A. Haylett, K. E. McKenna, R. Mallipeddi, H. Moseley, L. E. Rhodes, D. C. Seukeran, K. A. Ward, M. F. Mohd Mustapa, L. S. Exton, *Br. J. Dermatol.* **2019**, *180*, 715–729.
- [85] U. E. K. Schnurrbusch, C. Jochmann, W. Einbock, S. Wolf, *Arch. Ophthalmol.* **2005**, *123*, 1347.
- [86] M. Xu, L. Zhou, L. Zheng, Q. Zhou, K. Liu, Y. Mao, S. Song, *Cancer Lett.* **2021**, *497*, 229–242.
- [87] Z. Gong, Z. Dai, *Adv. Sci.* **2021**, *8*, 2002178.
- [88] N. Yumita, R. Nishigaki, K. Umemura, S. Umemura, *Jpn. J. Cancer Res.* **1989**, *80*, 219–222.
- [89] N. Yumita, K. Sasaki, S. Umemura, R. Nishigaki, *Jpn. J. Cancer Res.* **1996**, *87*, 310–316.
- [90] N. Yumita, R. Nishigaki, S. Umemura, *J. Cancer Res. Clin. Oncol.* **2000**, *126*, 601–606.
- [91] Y. Shen, J. Ou, X. Chen, X. Zeng, L. Huang, Z. Pi, Y. Hu, S. Chen, T. Chen, *BioMed Eng Online* **2020**, *19*, 52.
- [92] Y. Shen, Y. Chen, Y. Huang, X. Zeng, L. Huang, X. Diao, S. Chen, X. Chen, *Ultrasonics* **2021**, *110*, 106272.
- [93] H. Nesbitt, K. Logan, K. Thomas, B. Callan, J. Gao, T. McKaig, M. Taylor, M. Love, E. Stride, A. P. McHale, J. F. Callan, *Cancer Lett.* **2021**, *517*, 88–95.
- [94] X. Lin, R. Huang, Y. Huang, K. Wang, H. Li, Y. Bao, C. Wu, Y. Zhang, X. Tian, X. Wang, *Int. J. Nanomed.* **2021**, *16*, 1889–1899.
- [95] W. Um, P. Kumar, E. K. Y. Song, J. Lee, J. Y. An, H. Joo, D. G. You, J. H. Park, *Carbohydr. Polym.* **2021**, *273*, 118488.
- [96] M. M. Hadi, H. Nesbitt, H. Masood, F. Sciscione, S. Patel, B. S. Ramesh, M. Emberton, J. F. Callan, A. MacRobert, A. P. McHale, N. Nomikou, *J. Controlled Release* **2021**, *329*, 76–86.
- [97] T. G. Nguyen Cao, J. H. Kang, J. Y. You, H. C. Kang, W. J. Rhee, Y. T. Ko, M. S. Shim, *ACS Appl. Mater. Interfaces* **2021**, *13*, 25575–25588.
- [98] J. Huang, F. Liu, X. Han, L. Zhang, Z. Hu, Q. Jiang, Z. Wang, H. Ran, D. Wang, P. Li, *Theranostics* **2018**, *8*, 6178–6194.
- [99] T. Abduljabbar, F. Vohra, F. Javed, Z. Akram, *Photodiagn. Photodyn. Ther.* **2017**, *17*, 138–146.
- [100] A. Ahmad, A. Hayat, M. U. Rahman, J. Khan, *Am J Clin Microbiol Antimicrob* **2019**, *2*(3), 1041.
- [101] N. Kashef, M. R. Hamblin, *Drug Resist. Updates* **2017**, *31*, 31–42.
- [102] Y. Zheng, J. Ye, Z. Li, H. Chen, Y. Gao, *Acta Pharm. Sin. B* **2021**, *11*, 2197–2219.
- [103] G. Yaşa Atmaca, *Inorg. Chim. Acta* **2021**, *515*, 120052.
- [104] G. Y. Atmaca, C. C. Karanlık, A. Erdoğan, *Dyes Pigm.* **2021**, *194*, 109630.
- [105] N. Farajzadeh, G. Y. Atmaca, A. Erdoğan, M. B. Koçak, *Dyes Pigm.* **2021**, *190*, 109325.
- [106] W. Zhang, K. Li, J. Lu, Z. Peng, X. Wang, Q. Li, G. Zhao, J. Hao, Y. Luo, K. O'Brien, *Int J Complement Alt Med* **2017**, *9*.
- [107] M. Bakhshizadeh, T. Moshirian, H. Esmaily, O. Rajabi, H. Nassirli, A. Sazgarnia, *Iran. J. Basic Med. Sci.* **2017**, *20*, 10, 1088–1092.
- [108] Q. Li, X. Wang, P. Wang, K. Zhang, H. Wang, X. Feng, Q. Liu, *Cancer Biother. Radiopharm.* **2014**, *29*, 42–52.
- [109] P. Wang, C. Li, X. Wang, W. Xiong, X. Feng, Q. Liu, A. W. Leung, C. Xu, *Ultrason. Sonochem.* **2015**, *23*, 116–127.
- [110] M. Aksel, O. Bozkurt-Girit, M. D. Bilgin, *Photodiagn. Photodyn. Ther.* **2020**, *31*, 101909.
- [111] G. Y. Atmaca, M. Aksel, B. Keskin, M. D. Bilgin, A. Erdoğan, *Dyes Pigm.* **2021**, *184*, 108760.
- [112] Y. Liu, P. Wang, Q. Liu, X. Wang, *Ultrason. Sonochem.* **2016**, *31*, 437–448.
- [113] J.-X. Zhu, W.-T. Zhu, J.-H. Hu, W. Yang, P. Liu, Q.-H. Liu, Y.-X. Bai, R. Xie, *Ultrasound Med Biol* **2020**, *46*, 2030–2043.
- [114] A. A. Glowacka-Sobotta, B. D. Ziental, C. L. Sobotta, in *Smart Mater. Ser.* (Eds.: H. Lang, T. Rueffer), Royal Society Of Chemistry, Cambridge, **2021**, pp. 352–404.
- [115] J. Zhu, Y. Wang, P. Yang, Q. Liu, J. Hu, W. Yang, P. Liu, F. He, Y. Bai, S. Gai, R. Xie, C. Li, *Colloids Surf. B* **2021**, *197*, 111358.
- [116] E. Güzel, G. Y. Atmaca, A. E. Kuznetsov, A. Turkkol, M. D. Bilgin, A. Erdoğan, *ACS Appl. Bio Mater.* **2022**, *5* (3), 1139–1150.
- [117] M. Aksel, Ö. Kesmez, A. Yavaş, M. D. Bilgin, *J. Photochem. Photobiol. B* **2021**, *225*, 112333.
- [118] J. Musial, R. Krakowiak, D. T. Mlynarczyk, T. Goslinski, B. J. Stanisz, *Nanomaterials* **2020**, *10*, 1110.
- [119] F. Alves, G. Gomes Guimarães, N. Mayumi Inada, S. Prata Vieira, V. Salvador Bagnato, C. Kurachi, *Lasers Surg. Med.* **2021**, *53*, 1113–1121.

Manuscript received: April 3, 2022  
Revised manuscript received: April 28, 2022  
Accepted manuscript online: May 4, 2022  
Version of record online: May 23, 2022